Helsinki Medical Imaging Center
University of Helsinki
Finland

Department of Medicine / Division of Cardiology
University of Helsinki
Finland

Institute of Biomedicine / Department of Anatomy
University of Eastern Finland
Finland

Spectroscopy of tissue triglyceride composition

In vitro and in vivo studies

Jesper Lundbom

ACADEMIC DISSERTATION

To be presented, with the permission of the Faculty of Medicine of the University of Helsinki, for public examination in lecture room XII, University main building, on 18 December 2010, at 12 noon.

Helsinki 2010

Supervised by

Professor Markku Tammi, MD
Institute of Biomedicine, Department of Anatomy
University of Eastern Finland
Kuopio, Finland

Professor Marja-Riitta Taskinen, MD
Department of Medicine, Division of Cardiology
University of Helsinki
Helsinki, Finland

Reviewed by

Associate Professor Roland Kreis, PhD
Department of Clinical Research, Magnetic Resonance Spectroscopy and Methodology
University of Bern
Bern, Switzerland

Docent Satu-Pia Reinikainen, PhD
Department of Chemical Technology
Lappeenranta University of Technology
Lappeenranta, Finland

Official opponent

Docent Juhana Hakumäki, MD
Department of Clinical Radiology
Kuopio University Hospital
Kuopio, Finland

ISBN 978-952-92-8242-5 (pbk.)
ISBN 978-952-10-6715-0 (PDF)

Helsinki University Printing House
Helsinki 2010

Abstract

Lipid analysis is commonly performed by gas chromatography (GC) in laboratory conditions. Spectroscopic techniques, however, are non-destructive and can be implemented noninvasively *in vivo*.

Excess fat (triglycerides) in visceral adipose tissue and liver is known predispose to metabolic abnormalities, collectively known as the metabolic syndrome. Insulin resistance is the likely cause with diets high in saturated fat known to impair insulin sensitivity. Tissue triglyceride composition has been used as marker of dietary intake but it can also be influenced by tissue specific handling of fatty acids. Recent studies have shown that adipocyte insulin sensitivity correlates positively with their saturated fat content, contradicting the common view of dietary effects. A better understanding of factors affecting tissue triglyceride composition is needed to provide further insights into tissue function in lipid metabolism.

In this thesis two spectroscopic techniques were developed for *in vitro* and *in vivo* analysis of tissue triglyceride composition. *In vitro* studies (Study I) used infrared spectroscopy (FTIR), a fast and cost effective analytical technique well suited for multivariate analysis. Infrared spectra are characterized by peak overlap leading to poorly resolved absorbances and limited analytical performance. *In vivo* studies (Studies II, III and IV) used proton magnetic resonance spectroscopy (^{1}H-MRS), an established non-invasive clinical method for measuring metabolites *in vivo*. ^{1}H-MRS has been limited in its ability to analyze triglyceride composition due to poorly resolved resonances.

Using an attenuated total reflection accessory, we were able to obtain pure triglyceride infrared spectra from adipose tissue biopsies. Using multivariate curve resolution (MCR), we were able to resolve the overlapping double bond absorbances of monounsaturated fat and polyunsaturated fat. MCR also resolved the isolated *trans* double bond and conjugated linoleic acids from an overlapping background absorbance.

Using oil phantoms to study the effects of different fatty acid compositions on the echo time behaviour of triglycerides, it was concluded that the use of long echo times improved peak separation with T_2 weighting having a negligible impact. It was also discovered that the echo time behaviour of the methyl resonance of omega-3 fats differed from other fats due to characteristic J-coupling. This novel insight could be used to detect omega-3 fats in human adipose tissue in vivo at very long echo times (TE = 470 and 540 ms).

A comparison of ^{1}H-MRS of adipose tissue in vivo and GC of adipose tissue biopsies in humans showed that long TE spectra resulted in improved peak fitting and better correlations with GC data. The study also showed that calculation of fatty acid fractions from ^{1}H-MRS data is unreliable and should not be used. Omega-3 fatty acid content derived from long TE in vivo spectra (TE = 540 ms) correlated with total omega-3 fatty acid concentration measured by GC.

The long TE protocol used for adipose tissue studies was subsequently extended to the analysis of liver fat composition. Respiratory triggering and long TE resulted in spectra with the olefinic and tissue water resonances resolved. Conversion of the derived unsaturation to double bond content per fatty acid showed that the results were in accordance with previously published gas chromatography data on liver fat composition.

In patients with metabolic syndrome, liver fat was found to be more saturated than subcutaneous or visceral adipose tissue. The higher saturation observed in liver fat may be a result of a higher rate of de-novo-lipogenesis in liver than in adipose tissue.

This thesis has introduced the first non-invasive method for determining adipose tissue omega-3 fatty acid content in humans in vivo. The methods introduced here have also shown that liver fat is more saturated than adipose tissue fat.

Yleistajuinen tiivistelmä

Ylipaino, metabolinen oireyhtymä ja niihin liittyvä tyypin 2 diabetes yleistyvät nopeasti ja pelkästään Suomessa on arvioitu olevan noin 450 000 tyypin 2 diabeetikkoa. Metabolisen oireyhtymän ja siihen liittyvän tyypin 2 diabeteksen arvellaan olevan seurausta kehon heikentyneestä vasteesta insuliinihormonin vaikutuksille eli ns. insuliinresistenssistä. Paljon rasvaa ja sokeria sisältävä ruokavalio altistaa painonnousulle ja insuliiniresesistenssin kehittymiselle.

Aikaisempien tutkimusten perusteella paljon tyydyttyneitä ns. kovia rasvoja sisältävää ruokavaliota on pidetty haitallisena. Kovien rasvojen haitallisuudesta on kuitenkin esitetty eriäviä mielipiteitä ja aiheesta on käyty mediassa kiivasta keskustelua. Monityydyttämättömistä rasvoista erityisesti omega-3-rasvoja pidetään terveellisinä ja niitä myydään ravintolisävalmisteina. Ruokavalion omega-3-rasvojen vaikutusmekanismit ovat kuitenkin vielä epäselviä. Tutkimukset ruokavalion rasvan koostumuksen vaikutuksesta terveyteen ovat tuottaneet ristiriitaisia tuloksia. Ruokavalion tutkiminen on vaikeaa, sillä koehenkilöiden ruokavalion luotettava seuranta on käytännössä mahdotonta.

Rasva kerääntyy kehossa pääosin ihonalaiseen rasvakudokseen, jonka on siksi ajateltu edustavan ruokavalion rasvan koostumusta. Äskettäin on kuitenkin havaittu, että ihonalaisen rasvakudoksen kovat rasvat liittyvät hyvään insuliinin vaikutukseen rasvakudoksessa. Metabolisessa oireyhtymässä rasvaa kertyy myös viskeraaliseen rasvakudokseen ja maksaan.

Rasvan koostumus määritetään yleensä kudosnäytepaloista laboratorio-olosuhteissa. Viskeraalisen rasvakudoksen ja maksan rasvan tutkiminen vaatii siten kirurgista näytteenottoa vatsan sisäisistä kudoksista. Toimenpide on koehenkilölle hankala ja komplikaatioaltis, mikä on rajoittanut näiden erityisen haitallisten rasvakertymien tutkimista.

Spektroskopiamenetelmät mahdollistavat kemiallisen analytiikan tuhoamatta näytettä. Infrapunaspektroskopia (FTIR) on laajasti käytetty kemiallinen analyysimenetelmä, jonka spektrit soveltuvat hyvin monimuuttuja-analyysiin. Magneettiresonassispektroskopia (MRS) on kliininen menetelmä, joka mahdollistaa (koehenkilöön) kajoamattoman kemiallisen analyysin magneettikuvauslaitteella. Tässä väitöskirjatyössä FTIR- ja MRS-menetelmiä laajennettiin ihmisen kudosrasvan koostumuksen analysointiin.

FTIR-menetelmän käyttöä rasvakudoksen analyysissä rajoittaa spektrien analyyttisten piikkien huono erottuvuus toisistaan. Työssä parannettiin FTIR spektrien analyysiä soveltaen matemaattista monimuuttujamenetelmää. Työn tuloksena spektripiikkien erottelu parani ja niiden luotettava erottelu tuli mahdolliseksi. FTIR kykeni erottamaan rasvaspektristä trans- ja konjugoidut linolihapot, joiden analyysi perinteisillä menetelmillä on vaikeaa.

MRS-menetelmää kehitettiin ja sovellettiin koehenkilöihin, joilla on metabolinen oireyhtymä. Uudella MRS-menetelmällä pystyttiin analysoimaan ihonalaista ja viskeraalista rasvakudosta ja maksaan kertynyttä rasvaa. Yllättävä havainto oli, että maksaan kertyvä rasva on tyydyttyneempää kuin rasvakudoksen rasva. Uudella menetelmällä pystyttiin myös ensimmäistä kertaa määrittämään ihmisen rasvakudoksen omega-3- rasvoja kajoamattomasti.

Tässä väitöskirjatyössä kehitetyt kajoamattomat kudosrasvan analysointimenetelmät avaavat uusia mahdollisuuksia tutkia kudosrasvan koostumusta ja sen yhteyttä rasva-aineenvaihdunnan häiriöihin. Metabolisen oireyhtymän potilailla havaittu maksan rasvan korkea tyydyttyneisyys verrattuna rasvakudokseen saattaa olla seurausta muuttuneesta kudosten rasvahapposynteesistä.

Acknowledgements

This study was conducted at the University of Kuopio, Department of Anatomy and University of Helsinki, Division of Cardiology during the years 2004 to 2010. FTIR measurements were conducted at the Biomater Center in Kuopio and MRS measurements were conducted at HUS Medical Imaging Center in Helsinki. I wish to express my gratitude to Professor emeritius Heikki Helminen, former head of the Department of Anatomy and Professor Sauli Savolainen, Chief physicist at HUS Medical Imaging Center for allowing me to use their facilities for my research.

I am deeply grateful to my supervisor Professor Markku Tammi, MD for providing me with the support and opportunity to do research leading to this PhD thesis, educating me in all aspects of biological sciences, and believing in me despite a rocky start. I am equally grateful to my supervisor Professor emerita Marja-Riitta Taskinen, MD for her support, enthusiasm, and spirit, essentially pushing my research to the next level. I am indebted to my sister Docent Professor Nina Lundbom, MD for first introducing me to the fascinating world of magnetic resonance, her constant support throughout my research career, and acting as a third unofficial supervisor. I would also like to thank Docent Anna-Maija Häkkinen, PhD for my first lessons in the art of shimming a magnetic field. I am grateful to Associate Professor Roland Kreis, PhD and Docent Satu-Pia Reinikainen, PhD for reviewing the thesis.

I am thankful to everybody at the Department of Anatomy and the Biophysics of Bone and Cartilage group at the University of Kuopio for instantly making me feel as part of your group. I am still missing the parties and floorball matches. Special thanks go to Jarno Rieppo, MD for introducing me to FTIR measurement and spectral analysis techniques. I am grateful to Docent Marjukka Kolehmainen, PhD, Docent Ursula Schwab, PhD, Leena Pulkkinen PhD, and Professor Matti Uusitupa, MD for giving me access to all of their study data and generously providing valuable adipose tissue biopsies to my “risky” research. I am also grateful to Pasi Soininen, PhD and Mika Tiainen, MSc for taking on the demanding task of ^{1}H-NMR analysis of adipose tissue.

I am thankful to the whole staff of radiology technicians at HUS Medical Imaging Center for a positive attitude and understanding towards my unusual measurements. I am also grateful to the staff at the Helsinki University Division of Cardiology for their support and assistance in my research. Special thanks go to Pentti Pölönen, RT for excellent assistance in MR measurements of patients, creating a pleasant working environment, and saving my wallet from the trashcan. I am thankful to Jukka Westerbacka, MD and Sanni Söderlund, MD for professional patient handling and biopsies. Special thanks go to Docent Sami Heikkinen, PhD for valuable insights and comments on my thesis. I would also like to thank Antti Hakkarainen for being such a good MR collaborator, a fun working environment, and always being on board for any “crazy” MR experiments.

I would also like to extend my gratitude to all who donated adipose tissue biopsies to my research, not an entirely painless procedure. I am also grateful to the Savonheimo family, who helped me settle in Kuopio.

The biggest thanks and all my love go to my lovely Emilia and our daughter Svea-Louisa, who have provided my life with pure joy.

This study was financially supported by the TEKES program “Molecular Nutrigenomics Technologies”, HEPADIP EU FP6 program, Finnish Diabetes Association, Sigrid Juselius Foundation, Finnish Foundation for Cardiovascular Research, Instrumentarium Research Foundation, Paavo Nurmi Foundation, Orion-Farmos Research Foundation, and a special governmental subsidy for health sciences research from the Helsinki University Central Hospital.

Contents

List of original publications

This thesis is based on the following publications:

I Lundbom J, Kolehmainen M, Pulkkinen L, Soininen P, Tiainen M, Schwabb U, Uusitupa M, Tammi M. Mid-Infrared spectroscopy and multivariate curve resolution for analyzing human adipose tissue triacylglycerols. *European Jounal of Lipid Science and Technology*. Accepted for publication

II Lundbom J, Heikkinen S, Fielding B, Hakkarainen A, Taskinen M-R, Lundbom N. PRESS echo time behavior of triglyceride resonances at 1.5 Tesla: Detecting omega-3 fatty acids in adipose tissue in vivo. *Journal of Magnetic Resonance* 2009 Nov; 201(1): 39-47.

III Lundbom J, Hakkarainen A, Fielding B, Söderlund S, Westerbacka J, Taskinen M-R, Lundbom N. Characterizing human adipose tissue lipids by long echo time ^{1}H-MRS in vivo at 1.5 Tesla: validation by Gas Chromatography. *NMR in Biomedicine* 2010 Jun; 23(5):466-472.

IV Lundbom J, Hakkarainen A, Söderlund S, Westerbacka J, Lundbom N, Taskinen M-R. Long echo time ^{1}H-MRS suggests liver fat is more saturated than subcutaneous and visceral fat. *NMR in Biomedicine* (In press) DOI:10.1002/nbm.1580

The publications are referred to in the text by their roman numerals.

Author contribution:

The author designed the studies, carried out the FTIR and in vivo ^{1}H-MRS measurements, analyzed the data, and wrote the manuscripts. Fielding B, PhD carried out gas chromatography measurements in Studies II and III. Heikkinen S, PhD carried out the *in vitro* ^{1}H-NMR measurements in Study II. Soininen P, PhD and Tiainen M carried out the *in vitro* ^{1}H-NMR measurements in Study I. Adipose tissue biopsies were provided by Uusitupa M, MD for Study I. Westerbacka J, MD and Söderlund S, MD collected adipose tissue biopsies for Study III and recruited patients for Study IV. Mr Antti Hakkarainen assisted in in vivo ^{1}H-MRS measurements of Study III, and segmented MR images of fat distribution in Study IV.

Abbreviations

AMARES	Advanced method for accurate, robust, and efficient spectral fitting
ALS	Alternating Least Squares
ATR	Attenuated total reflection
BMI	Body Mass Index
CLA	Conjugated linoleic acids
COSY	Correlation Spectroscopy
CVD	Cardiovascular disease
DB/FA	Double bonds per fatty acid chain
DNL	De-novo lipogenesis
FAME	Fatty acid methyl ester
FFA	Free fatty acids
FID	Free induction decay
FTIR	Fourier transform infrared
GC	Gas Chromatography
HDL	High density lipoprotein
LDL	Low density lipoprotein
MCR	Multivariate curve resolution
MRI	Magnetic resonance imaging
MRS	Magnetic resonance spectroscopy (refers to in vivo NMR spectroscopy)
MUFA	Monounsaturated fatty acids
NAFLD	Non-alcoholic fatty liver disease
NMR	Nuclear magnetic resonance
PCA	Principal component analysis
PRESS	Point resolved spectroscopy sequence
PUFA	Polyunsaturated fatty acids
SAFA	Saturated fatty acids
SAT	Subcutaneous adipose tissue
STEAM	Stimulated echo acquisition mode
STIR	Short T_1 inversion recovery
T_1	Longitudinal relaxation time
T_2	Transverse relaxation time
T2D	Type 2 diabetes
TE	Echo time
TG	triglyceride (triacylglyceride)
TMS	Tetramethylsilane
TR	Repetition time
VOI	Volume of interest
ω	omega (omega notation of fatty acids)
ω	angular frequency

1 Introduction

Lipids play a major role in a wide variety of biological processes from cellular signalling to health effects of dietary intake in humans. Analysis of the multitude of different lipid molecules and their incorporation into different molecular complexes requires specialized methods. Gas chromatography (GC) was developed largely by lipid scientists for analysing lipid composition (Christie 1989). To this day, gas chromatography, albeit with much improved techniques, is still the standard for determining the fatty acid composition of lipids.

Spectroscopy encompasses multiple analytical techniques with the common characteristic of observing the interaction of electromagnetic waves with matter and, as such, do not require the studied sample to be destroyed. Thus spectroscopic techniques can be implemented non-invasively, a significant advantage for human studies.

Excess accumulation of adipose tissue, or obesity, is a major health risk and increasing in prevalence (Kopelman 2000). Serious adverse complications of obesity are type 2 diabetes (T2D) and cardiovascular disease (CVD). Although the development of obesity is easily attributed to excess intake of calories (Drewnowski 2007), the underlying reasons for the metabolic disturbances and health risks associated with obesity are still unclear. It is known that the distribution of adipose tissue plays a major role in the development of T2D and CVD, with central obesity associated with increased risk of developing these disorders.

Metabolic syndrome is the clustering of specific risk factors and is associated with T2D and CVD (Alberti *et al*. 2005). Central obesity, measured as waist circumference, is a requirement for its diagnosis, and functions as a marker of visceral adipose depot size. This enlarged depot supplies the liver with a high flux of non-esterfied fatty acids, suggested to lead to fatty liver (Lewis *et al*. 2002). Fat accumulating in the liver, or Non-alcoholic fatty liver disease (NAFLD), is also strongly associated with the metabolic syndrome and may be responsible for many of the metabolic disturbances, e.g. dyslipidemia and glucose intolerance (Szendroedi *et al*. 2009).

Numerous positive and negative health effects have been attributed to specific dietary fats (Seidelin 1995). Using self reporting to study dietary habits is, however, prone to errors (Lichtman *et al*. 1992). Human subcutaneous adipose tissue stores excess energy as triglycerides and has therefore served as a marker of dietary fat composition in studies on health effects of dietary fats (Arab 2003). Dietary intake, however, only partly explains the lipid composition of human adipose tissue (Seidelin 1995). Remarkably, recent studies have shown that adipocyte saturated fat content correlates positively with insulin sensitivity (Sjögren *et al*. 2008, Roberts *et al*. 2009). How different types of fat are distributed among the subcutaneous, visceral, and liver depots, and how this relates to insulin resistance, is still an open question.

Conventional methods of analysing lipid composition rely on the analysis of extracted tissue samples. The extraction and subsequent sample handling is invasive and may introduce errors and limit possible applications. Spectroscopic techniques can circumvent the extraction and/or the sample modification inherent to invasive techniques.

The aim of this thesis was to develop new spectroscopic methods for analysing lipid composition. The spectroscopic techniques chosen for further development were Fourier transform infrared spectroscopy (FTIR) and proton magnetic resonance spectroscopy (^{1}H-MRS). Infrared spectroscopy provides fingerprints of specific molecular vibrations and is well suited for multivariate analysis (Schoonover *et al*. 2003). *In vivo* magnetic resonance spectroscopy is non-invasive but currently limited in its performance in analysis of lipid composition (Boesch *et al*. 2006). Specifically, here both spectroscopic techniques were developed and applied to the analysis of human fat in relation to obesity and metabolic syndrome with the aim of determining tissue differences in fat composition.

2 Background

2.1 Lipids, triglycerides and fatty acids

Lipids are one of the four major building blocks of the cell, with phospholipids forming the lipid bilayer of the outer membrane. Sterols, like cholesterol, are also abundant in cell membranes, providing rigidity, but also act as a signalling and hormone precursor molecules. Triglycerides are a group of lipids with the major function of serving as an energy reservoir. Many other molecules are also classified as lipids; ceramides, fatty acids, sphingolipids, glycolipids, all with specific biological functions.

The general common characteristic of lipids is that they are readily soluble in organic solvents. Using the solubility as a definition for lipids has been criticized as unnecessarily broad. William W. Christie has proposed the following definition for lipids: ”*Lipids are fatty acids and their derivatives, and substances related biosynthetically or functionally to these compounds*” (Christie 1989). This definition highlights the importance of fatty acids as the central lipid compounds.

Triglycerides consist of a glycerol backbone with three fatty acids attached, forming a non-polar lipid molecule. As non-polar intermediate sized molecules triglycerides are non-toxic, insoluble in water, and usually deposited as lipid droplets in the cytoplasm. Triglycerides form more than 90 % of adipose tissue, which is the primary triglyceride reservoir in humans. Triglycerides are also the main constituents of edible oils and fat.

Fatty acids are straight chains of carbon atoms with a carboxyl group at one end and a methyl group at the other end. The carbon chains in human fatty acids span 14 to 22 carbons in length, always with an even number of carbons. The carbons may be attached by single or double bonds, with double bonds usually in the *cis*-configuration although *trans*-configurations also occur. Fatty acids with no double bonds are saturated (saturated fatty acids, SAFA), with one double bond monounsaturated (monounsaturated fatty acids, MUFA), and with more than one double bond polyunsaturated (polyunsaturated fatty acids, PUFA). The fatty acids can also be characterized according to the position of the first double bond counting from the methyl end, i.e. the ω notation.

The health effects of dietary fats have received much attention. Polyunsaturated fatty acids (PUFA) α-linolenic acid (ω-3) and linoleic acid (ω-6) cannot be synthesized by humans and are essential dietary nutrients required for proper metabolism. Although the modern western diet has made PUFA deficiency virtually non-existent, recent studies have suggested that the low dietary ω-3 / ω-6 ratio is a potential health hazard (Ailhaud *et al*. 2006). The ω-3 and ω-6 fatty acids take part in complex cascades competing for elongase and desaturase enzymes, with ω-6 fatty acids generally forming more inflammatory end products. The adverse health effects of dietary saturated and *trans* fatty acids have been mainly attributed to their ability to raise blood cholesterol levels. *Trans* fatty acids are considered especially harmful as they increase the atheropromoting Low-density lipoproteins (LDL) and lower the atheroprotective High-density lipoproteins (HDL) (Mozaffarian *et al*. 2006).

2.2 Fourier transform infrared spectroscopy

Infrared spectroscopy is a widely used analytical technique introduced for determining isolated *trans* isomers in oils and fats in the 1940's.

2.2.1 Infrared spectroscopy

Infrared spectroscopy detects absorption of specific frequencies of electromagnetic radiation, with the most commonly used mid-infrared spectrum spanning the wavenumbers 4000–400 cm^{-1} (wavelengths 30–2.5 μm).

As a molecule absorbs radiation at a specific frequency, it produces a peak in the infrared spectrum at the corresponding wavenumber. The modes of vibration in a molecule that can absorb infrared radiation are many and increase with increasing complexity of the molecule. The only restriction is that the vibration mode has to have a changing dipole moment, which the radiation can couple to. The vibrations that contribute to the spectrum are bending and stretching vibrations between atoms and rocking, twisting and wagging of a functional group. These modes can couple with each other and the rotational motion of the whole molecule to produce very complex spectra.

Although the frequency, at which a chemical bond absorbs infrared radiation, is to a high degree affected by external factors (temperature, hydration state, solute etc.), the functional groups of organic molecules have relatively stable characteristic frequencies.

These functional group frequencies occur in the wavenumber region 4000-1500 cm^{-1}, also called the functional group region, and can be used to identify the molecular composition of the sample (Griffiths *et al*. 1986).

The region below 1500 cm^{-1} is called the fingerprint region and contains absorptions of skeletal vibrations that are difficult to assign to specific vibrational modes. These skeletal vibrations are for the most part unique for each molecule and enable the identification of unknown molecules through correlation with existing standard spectra.

2.2.2 ATR-FTIR

Fourier transform infrared spectroscopy (FTIR) is based on the Michelson interferometer. By splitting the infrared beam in two directions and subsequently merging them with a moving mirror at varying optical path differences, produces an interferogram. When the optical path difference of the two beams equals half of the wavelength, interference cancels out the signals, while at zero optical path difference a signal maximum is observed. For monochromatic radiation, the interferogram observed at the detector would correspond to a single cosine wave, given by the equation

$$I_D(\delta) = \frac{I_S(\nu)}{2}\left[1 + \cos(2\pi\nu\delta)\right]. \quad (1)$$

Here I stands for the intensity, with the subscripts S for source and D for detector, δ is the retardation of the moving mirror and ν is the frequency of the monochromatic radiation (Griffiths *et al.* 1986). In the polychromatic case one integrates over the whole frequency range. The interferogram obtained in this way is Fourier transformed from the retardation domain to the wavenumber domain to obtain the infrared spectrum.

Attenuated total reflection (ATR) is a specialised sampling technique that, when coupled with FTIR, can be used to obtain the infrared spectrum of solid or liquid samples in their native state. The ATR setup consists of an ATR crystal, upon which the sample is placed. An infrared beam is passed through the ATR crystal, reflects of the interface of the crystal and the sample, and is passed through to the detector. During the reflection, an evanescent wave extends beyond the crystal into the sample, which enables the absorption of infrared frequencies by the sample (Figure 1). The penetration depth of the evanescent wave is a function of wavelength with deeper penetration at longer wavelengths. This may lead to distortions in the relative intensities of infrared peaks if sample thickness is insufficient for complete coverage of the evanescent wave. (Goormaghtigh *et al.* 1999)

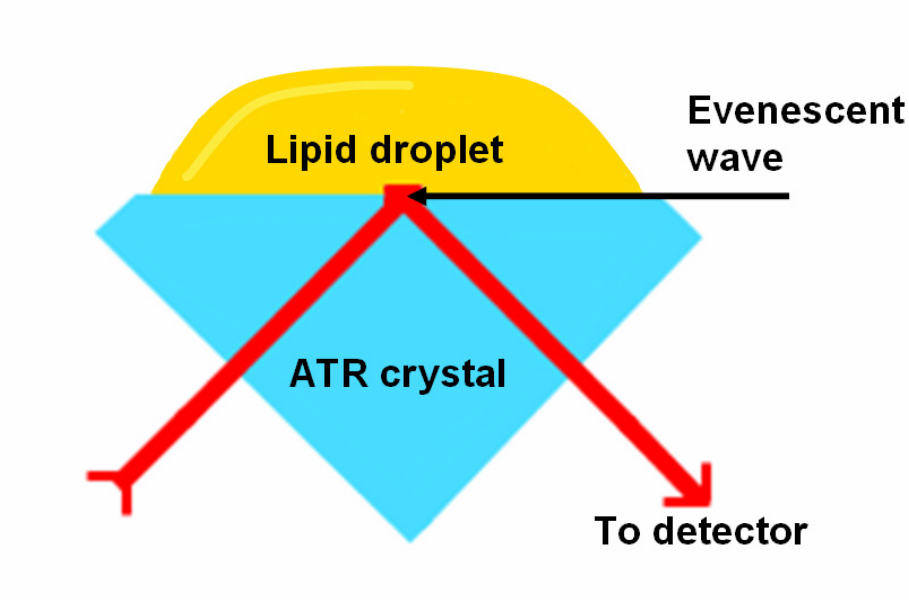

Figure 1 *Schematic function of the ATR setup. The infrared beam is directed through the crystal and reflected of the interface with the sample (a lipid droplet). The evanescent wave extends into the sample and infrared absorption occurs, which is observed in the detected infrared beam.*

2.2.3 FTIR of lipids

Vibrational spectroscopy has been used as a fast and non-destructive alternative to GC in the analysis of lipids in the food industry. Specifically, FTIR (Guillen *et al.* 1997, Yang *et al.* 2005), FT-Near Infrared (Li *et al.* 2000, Cen *et al.* 2007) and FT-Raman (Baeten *et al.* 1998) spectroscopy have been used to study edible oils and fats.

Mid-infrared spectroscopy was found to be a useful tool for determining isolated *trans* isomers, assigned to the peak at 966 cm^{-1}, in fats already in the 1940s (van de Voort *et al*. 2001). With the advantages provided by the new FTIR spectrometers and new sampling methods, such as ATR, the analysis of oils and fats by vibrational spectroscopy has been extended to include characterization of oils and fats (Guillen *et al*. 1998), detecting oil adulteration (Lai *et al*. 1994) and monitoring oil oxidation (Guillen *et al*. 1999). Detection of oil adulteration has concentrated on detection of high quality olive oil adulteration by sunflower or hazelnut oil, and been implemented mainly through multivariate methods (Guillen *et al*. 1998, Ozen *et al*. 2002). The progression of oil oxidation and the formation of oxidation products can be monitored by changes in specific peaks in the infrared spectrum. During the first stages of oxidation the formation of hydroperoxides can be monitored by the appearance of a broad peak around 3450 cm^{-1}. Later on in the oxidation process the disappearance of *cis* double bonds can be seen around 3006 cm^{-1} and the appearance of various oxidation products at different wavelengths (Guillen *et al*. 1999).

In FTIR of oils and fats, several peaks and their exact frequencies or band ratios have been used as markers of TG fatty acid composition (Guillen *et al*. 1998). However, few peaks can be attributed to a specific class of fatty acids (Guillen *et al*. 1997). Consequently, FTIR has been mainly used to characterize fats and oils rather than for determining the exact fatty acid composition. The most popular measured characteristics of oils and fat have been the iodine value (IV), determined from the *cis* double bond peak at 3006 cm^{-1} (Guillen *et al*. 1997), and *trans* FA content, determined from the peak area at 966 cm^{-1} (Adam *et al*. 1999). Also the amount of free fatty acids (FFA) in oil samples have been determined by assigning the peak at 1744 cm^{-1} to the carbonyl of triglyceride esters and the peak at 1711 cm^{-1} to the carbonyl of FFA (Ismail *et al*. 1993).

Recent studies have indicated that the exact peak position of the *cis* double bond peak is sensitive to the amount of double bonds in the fatty acid chain (Yoshida *et al*. 2004). Also, a background vibration located near the isolated *trans* isomer peak has been found to influence the determination of *trans*FA content at low *trans* concentrations (Mossoba *et al*. 2007).

2.2.4 Analysis of infrared spectra

Infrared spectroscopy is a quantitative method. The amount of radiation transmitted through the sample is directly proportional to the total number of molecules in the beam path, as stated by Beer's law. Lambert's law states that the proportion of energy absorbed by the sample is independent of the intensity of the incident radiation. The Beer-Lambert law describes the relationship between the absorbed radiation and the sample concentration;

(2) $A = \varepsilon c l$.

Here c is the concentration in grams molecules per liter, l is the light path in centimeters and ε is the molar absorption coefficient of the substance expressed in liters per mole per centimeter (Griffiths *et al*. 1986).

According to equation 2, a peak in the infrared spectrum known to originate from the vibration of a specific molecule can be used to quantify its concentration. The area under the peak determines the total absorbance of the vibration and can be estimated by curve fitting, direct area evaluation, and multivariate methods. Direct area evaluation is appropriate when the peak in question is well resolved. If, as is often the case, there are overlapping peaks, curve fitting and multivariate methods are a better choice.

Multivariate methods used to analyze infrared spectra include clustering, principal component analysis (PCA) and multivariate curve resolution (MCR). Clustering uses the similarities and dissimilarities of spectra to assign samples to distinct groups for example in taxonomy of bacteria (Naumann *et al*. 1991) and classification of tissue structures (Fabian *et al*. 2002). Principal component analysis is a dimension reduction method used to reduce the information content of the spectra into principal components (PC) that maximally describe the underlying variance in the data set (Gemperline 2006). The obtained PCs are determined by the variance in the data set and thus do not represent chemically meaningful information. MCR factorizes the data matrix **D** into the product of two matrices **C** (concentrations) and $\mathbf{S}^{\mathbf{T}}$ (pure spectra) and the residual matrix **E**.

(3) $\mathbf{D} = \mathbf{C}\mathbf{S}^{\mathbf{T}} + \mathbf{E}$.

In contrast to PCA, the concentrations (**C**) obtained by MCR can be considered chemically meaningful as they correspond to associated pure spectra ($\mathbf{S}^{\mathbf{T}}$). The pure spectra derived by MCR may, however, be a non-chemical entity depending entirely on the used data set. Due to rotational and scale ambiguity problem associated with factorization, the MCR results are not unique (Tauler *et al*. 1995). This problem can be alleviated by imposing constraints and initial estimates on the possible solutions (de Juan *et al*. 1997). Commonly used constraints in spectroscopic data are non-negativity of concentrations and pure spectra. Another problem with MCR is rank deficiency, which arises when the number of PCs in the data set is less than the number of spectrally distinct species (Tauler *et al*. 1995). This means that MCR cannot resolve all distinct signals in the data set. The number of components to be used for MCR can be estimated from the data set by PCA as a preprocessing step.

If the spectral profiles of the compounds contributing to the spectra are known, the MCR algorithm should provide pure spectra corresponding to the spectral profiles of the known compounds.

2.3 Magnetic resonance spectroscopy

2.3.1 Nuclear magnetic resonance

Protons possess a purely quantum mechanical intrinsic angular momentum or spin, characterized by the spin quantum number I = ½. According to quantum mechanics, the direction of the spin can only be specified in one direction at a time, usually denoted the z-direction. When this direction is specified by an external magnetic field, the spins will align themselves parallel (½) or anti-parallel (-½) to the field, with the population difference of the spin states creating a net magnetization. The spins precess around the magnetic field with the Larmor equation

$$\omega = \gamma B, \tag{4}$$

giving the angular resonance frequency ω of the spins in a given magnetic field B, related by the gyromagnetic ratio γ.

For a sample in a magnetic field $\mathbf{B_0}$ the spins precess at random phase, i.e. without coherence, creating an observable net magnetization $\mathbf{M_Z}$ in the direction of the magnetic field. In order to observe the magnetization of the sample, an excitation pulse $\mathbf{B_1}$ is used to perturb the steady state and ”flip” the magnetization perpendicular to the main magnetic field, creating phase coherence of the spins and thus transverse magnetization $\mathbf{M_{XY}}$. The process of creating transverse magnetization can be rationalized by classical as well as quantum mechanics. In the classical picture, the magnetization $\mathbf{M_Z}$ spirals down to the transverse plane under the influence of the alternating $\mathbf{B_1}$ magnetic field. The Bloch equations, introduced by Felix Bloch (Bloch 1946), mathematically describe the behaviour of the magnetization under the influence of the magnetic fields.

2.3.2 Relaxation

After excitation of the magnetization $\mathbf{M_Z}$ to $\mathbf{M_{XY}}$, the magnetization will start to return to the steady state through relaxation processes. The return of the longitudinal magnetization is called spin-lattice relaxation and characterized by the time constant T_1. The disappearance of the transverse magnetization is called spin-spin relaxation and characterized by the time constant T_2. As indicated by the names, different physical processes underlie these two relaxation concepts.

The microscopic relaxation process is governed by the interaction of the spin with the surroundings (lattice) or nearby spins. Relaxation occurs when the spin changes its orientation relative to the magnetic field and loses coherence. The most common relaxation process is the magnetic dipole-dipole interaction, depicted by the Bloembergen-Purcell-Pound theory (Bloembergen *et al.* 1948). According to this theory any magnetic field fluctuating with a frequency near the Larmor frequency will induce a transition in the state of the spin. In liquid systems, molecular tumbling causes the spins with magnetic

moments to generate randomly varying magnetic fields, which neighbouring spins sense as radiofrequency fields and can induce transitions when at Larmor frequency. Theoretical analysis of the dipole-dipole relaxation pathway enables the derivation of analytical expressions for the T_1 and T_2 relaxation components, although these only apply to ideal conditions. An important feature of the Bloembergen-Purcell-Pound theory is that it can accurately describe and predict the effects of molecular mobility and magnetic field strength on relaxation in simple liquids. Analytical analysis of T_2 relaxation shows that T_2 increases with increasing molecular mobility (decreasing viscosity) (Bloembergen *et al*. 1948). An important consequence of the mobility dependence of T_2 is that immobile molecules cannot be observed by ^{1}H-MRS due to their very short T_2.

The transverse magnetization $\mathbf{M_{XY}}$ can be observed as it induces an electromotive force in a coil placed near the sample perpendicular to the main magnetic field. As the transverse magnetization decays it produces a Free Induction Decay (FID). The FID decays with the time constant T_2*, as magnetic field inhomogeneities also contribute to the loss of phase coherence.

2.3.3 *In vivo* ^{1}H-NMR Spectroscopy (^{1}H-MRS)

The chemical shift effect enables NMR spectroscopy, as protons with different positions on the molecule may experience small shifts in their surrounding magnetic field and hence their Larmor frequency. The electron cloud of the molecule shields the protons from the main magnetic field causing a slight decrease in the magnetic field strength observed by the proton. Fourier transform of the FID provides a spectrum with all frequencies within the sample, and enables identification of chemically distinct protons according to their characteristic frequencies. Due to the exponential decay of the FID, the Fourier transform will produce Lorentzian lineshapes with the peak position indicating resonance frequency of the spins. In practice, ideal lineshapes are not observed *in vivo*, due to motion artefacts, frequency drift, susceptibility effects, peak overlap, and J-coupling.

For *in vivo* applications, localization of the signal is generally required. This is usually achieved by sampling an echo. The spin echo, first proposed by Hahn (Hahn 1950), is created by first flipping the magnetization into the transverse plane with a so called 90° pulse and letting the $\mathbf{M_{XY}}$ dephase. After a time period TE/2 an inversion pulse, also called 180° pulse, is applied, which after another time period TE/2 creates an echo. The total time from the 90° pulse to the observed echo is thus TE, and called echo time. In essence, the echo is formed as the dephased spins are rephased by the inversion pulse. As the spin echo refocuses dephasing due to magnetic field inhomogeneities, the signal will decay during TE by T_2-relaxation processes. By varying the echo time in a spin echo experiment, the observed decay rate will be characterized by the true T_2-relaxation time constant, although diffusion and J-modulation may also affect the decay rate.

The point resolved spectroscopy sequence (PRESS), created by Bottomley (Bottomley 1984), uses two inversion pulses in combination with localization gradients to localize the arising spin-echo to a three dimensional volume of interest (VOI). PRESS has become the

most widely used localization technique in clinical proton MRS, pulse sequence presented in Figure 2. Another widely used localization sequence in *in vivo* ^{1}H-MRS is STEAM (STimulated Echo Acquisition Mode), which can reach shorter echo times than PRESS, but can only collect half of the signal (Frahm *et al*. 1987).

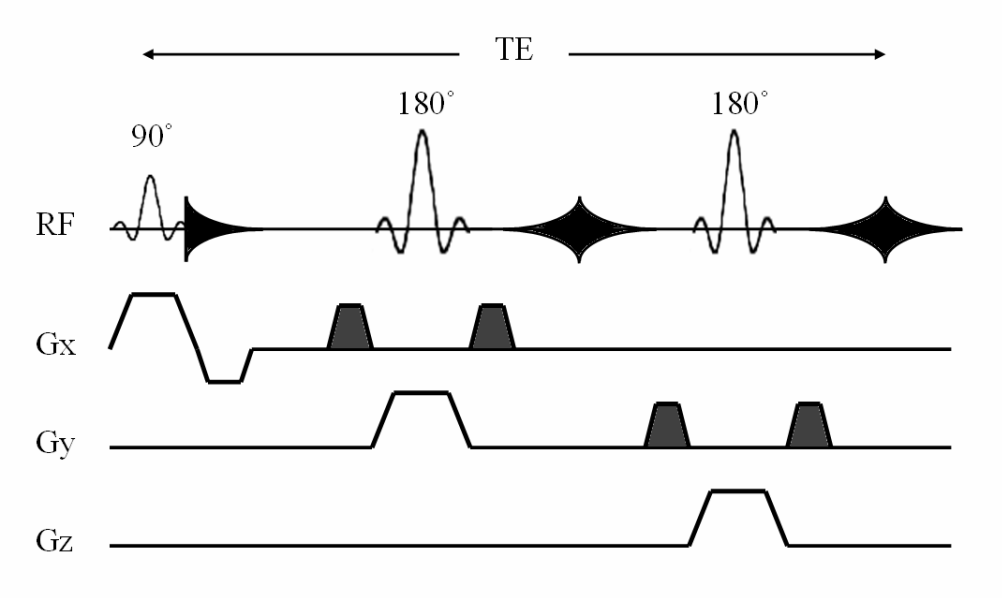

Figure 2 *The scheme of PRESS. The top row shows the timing of the RF-pulses and the three bottom rows show the timing of the three linear gradients **Gx**, **Gy** and **Gz** synchronized to the RF-pulses. Crusher gradients are dark. The time from the excitation (90˚) pulse to the acquired echo is the echo time (TE).*

2.3.4 J-Coupling

The spins of non-equivalent protons can couple through interaction with the bonding electron cloud (Ramsey *et al*. 1952), a phenomenon known as J-coupling. For ½-spins the resonance of a spin A will be split into N+1 resonances, when coupled with N magnetically equivalent spins X, forming a so called AX_N spin system. The impact J-coupling has on the NMR spectrum depends on the frequency difference between resonances A and X $|\nu_A-\nu_X|$ in relation to the J-coupling present between the resonances. J-coupling is measured as the frequency difference between resonances in a multiplet and is denoted J (Hz). When $|\nu_A-\nu_X|$ is much larger than J the spin system is said to be first order. When the frequency difference of the two spins is of the same order with J, the spin system exhibits second order effects i.e. is said to be strongly coupled. This kind of two-spin system is typically denoted as an AB spin system. Although $|\nu_A-\nu_X|$ scales with the strength of the magnetic field, J is independent of magnetic field strength.

The inversion pulse in the spin echo experiment will lead to refocusing of the chemical shift evolution as well as refocusing of the magnetic field inhomogeneities. However, the inversion pulse does not refocus the evolution of J in the homonuclear spin system, since both spins are affected. This leads to a phase difference ($\Delta\varphi$) between the resonance lines

determined by the length of TE. For a first order resonance doublet the TE dependence of the phase difference is given by the equation

(5) $\Delta\phi = \pi JTE$.

This leads to J-modulation of the multiplet structure, which is not automatically refocused in the echo (de Graaf 1998). A resonance doublet, exhibiting first order effects, will be refocused by the spin echo when TE = 2/J. A common example of this phenomenon is the lactate doublet at 1.33 ppm, which can be refocused with TE = 288 ms (J = 6.97 Hz). More complex second order spin systems exhibit complex J-evolution, which can be studied experimentally or with simulation runs. All triglyceride protons exhibit some degree of J-coupling.

2.3.5 ^{1}H-NMR of lipids

In vivo ^{1}H-MRS has been widely used to measure the intramyocellular- (IMCL) (Boesch *et al*. 1997) and intrahepatocellular lipid content (IHCL) (Szczepaniak *et al*. 1999). The lipids are observed as the methylene resonance of triglycerides, resonating at 1.3 ppm. Lipids bound to membranes and proteins do not generate an NMR visible signal, as the T_2 of these species are extremely short due to the rigid surroundings. For example, in healthy brain no lipid resonances are observed. In fact, an observable lipid signal in the brain can be attributed to cell destruction or apoptotic processes (Hakumaki *et al*. 1999).

There are a limited number of studies using ^{1}H-NMR to measure lipid composition, mainly as the proton NMR spectrum of lipids has limited analytical capabilities. High field *in vitro* ^{1}H-NMR spectroscopy has been used to study the composition of tissue lipids (Willker *et al*. 1998, Oostendorp *et al*. 2006) and edible oils and triglycerides (Guillén *et al*. 2003, Knothe *et al*. 2004, Sacchi *et al*. 1997, Lie Ken Jie *et al*. 1995).The *in vitro* ^{1}H-NMR spectrum provides information on chemically distinct protons in the triglycerides, but generally does not resolve individual fatty acids. Indirectly, through using the known proton contributions to individual peaks, also the MUFA, SAFA and PUFA ratios have been calculated (Knothe *et al*. 2004). The methyl resonance of the ω-3 fatty acids is well resolved in high field *in vitro* ^{1}H-NMR spectroscopy (Guillén *et al*. 2003), but has not yet been observed *in vivo*.

The low magnetic field strengths used in human *in vivo* ^{1}H-MRS reduces the spectral dispersion and imposes limits on using the proton spectrum for analysis of lipid composition. In humans ^{1}H-MRS at 1.5 Tesla, has been used to study the unsaturation of bone marrow fat using the olefinic resonance at 5.3 ppm (Yeung *et al*. 2005), and a methylene-to-methyl resonance ratio (CH_2/CH_3) has been derived for IMCL from long echo time spectra (TE = 270 ms) (Skoch *et al*. 2006). Recently, ^{1}H-MRS was used to measure human adipose and marrow fat composition with a 7 Tesla *in vivo* MR imager (Ren *et al*. 2008).

In magnetic resonance imaging adipose tissue is mainly a source of artifacts to be suppressed. Short T_1 inversion recovery (STIR) can be used to suppress fat by nulling fat

magnetization with an inversion pulse before a sequence, as the T_1 of fat is short compared to tissue water (≈220ms at 1.5 Tesla). The short T_1 in fat mainly applies to methylene protons of the triglycerides, which are the largest contributors to the *in vivo* fat signal. Longer T_1 constants have been measured for olefinic T_1 = 400ms and methyl protons T_1 = 750ms in bone marrow *in vivo* (Schick 1996). Measuring the true T_2 of lipids is difficult as a simple spin echo sequence will invariably be influenced by J-coupling present in all triglyceride resonances. The methylene resonance does, however, present an exponential decay rate and has been used to derive an apparent T_2 constant for bone marrow triglycerides (Schick 1996).

2.3.5 Analysis of ^{1}H-NMR spectra

The intensity (the peak area) of the resonance observed in an NMR spectrum is directly proportional to the concentration of spins contributing to the observed resonance. To obtain molar concentrations of specific compounds, numerous correction factors have to be taken into account. Factors other than spin concentration affecting resonance intensity are; T_1 and T_2 relaxation effects, coil loading, RF-field nonuniformities, voxel volume, temperature, J-coupling, nuclear Overhauser effect, and diffusion (de Graaf 1998). Some of these effects can be cancelled out using resonance ratios.

Estimating the intensity of an *in vivo* NMR resonance is no trivial task. Low magnetic field strengths increase peak overlap, and sample specific perturbation of the magnetic field lead to fairly large differences in obtainable spectral linewidths (homogeneity). These problems lead to severe uncertainty in obtaining a reliable fit of resonance areas i.e. intensities. As an example, the widely used fitting software LCmodel® uses a 20% standard deviation as a criterion of acceptable fit (Provencher 2008). This would suggest that only changes exceeding 40% of original intensity can be reliably observed. The LCmodel software uses a linear combination of measured and simulated spectral basis sets for complete analysis of the measured spectrum.

The jMRUI software has been developed for analysing *in vivo* NMR spectra and is freely available to academia [www.mrui.uab.es/mrui/]. Fitting algorithms in jMRUI v3.0 include AMARES (Advanced Method for Accurate, Robust and Efficient Spectral fitting) (Vanhamme *et al*. 1997) and QUEST (Ratiney *et al*. 2005). AMARES is an extension of VARPRO (Variable Projection method) and uses a sophisticated nonlinear least-squares algorithm to minimize the general functional. In addition, AMARES enables the use of constraints in order to impose prior knowledge in the analysis. QUEST uses measured or simulated basis spectra for complete analysis of the spectrum, as in LCmodel.

AMARES and QUEST use the time-domain signal to analyse the spectrum, while LCmodel analyses the frequency-domain. Although theoretically equivalent (Vanhamme *et al*. 2001), the frequency domain analysis may perform better on *in vivo* signals with variable baselines.

2.4 Obesity and Metabolic syndrome

Obesity is the accumulation of excess adipose tissue and, although a normal physiological process, will over time predispose to severe conditions such as osteoarthritis, cancer, type 2 diabetes, and cardiovascular disease (Manson *et al*. 1990). Obesity develops gradually when energy consumption exceeds energy expenditure (Drewnowski 2007). Obesity is defined as a body mass index (BMI) > 30 kg/m^2 although this does not take into account body composition.

Adipose tissue accumulating in the intra-abdominal cavity is considered especially harmful, as it has been linked to multiple cardiometabolic risk factors. Abdominal obesity has long been known to be related to the risk of cardiovascular disease (CVD). Studies have shown that the risk factors for CVD tend to cluster together, with this cluster nominated the metabolic syndrome. Although different criteria exist for the diagnosis of metabolic syndrome, they share the common requirements of existence of abdominal obesity and indications of dyslipidemia and impaired glucose tolerance. Insulin resistance has been proposed as the underlying factor accounting for the metabolic disturbances seen in metabolic syndrome (Reaven 1988).

2.4.1 Adipose tissue

Adipose tissue stores excess energy as triglycerides in adipocytes and was long considered a passive storage depot with little interest beyond the depot size. Adipose tissue has since been shown to be an active endocrine organ, excreting hormones and cytokines, with important physiological roles. Leptin, a hormone released by adipose tissue, is known for its ability to suppress appetite and also acts as an adiposity signal (Considine *et al*. 1996). Adiponectin, a hormone also released by adipose tissue and regulator of metabolism, is in contrast decreased in obesity (Fang *et al*. 2006).

Adipose tissue continuously takes up from and releases fatty acids into the blood stream. Liver derived lipoproteins are hydrolyzed by lipoprotein lipase action, releasing free fatty acids (FFA) that are taken up by adipocytes and esterfied into triglycerides. Fatty acids are freed from the triglycerides through the action of adipose triglyceride lipase (Zimmermann *et al*. 2004) and hormone sensitive lipase (HSL), and bound to album for transportation in the circulation.

Insulin is a potent anti-lipolytic hormone. In the insulin resistant state, the body is unable to suppress adipose tissue lipolysis, which leads to a high release of FFA. Especially visceral adipocytes are more susceptible to release FFA and less responsive to anti-lipolytic hormones (Wajchenberg 2000). The FFAs released by visceral adipose tissue are directly deposited in the portal blood stream leading to the liver.

2.4.2 Liver

The liver has a central role in regulating lipid and carbohydrate metabolism of the human body. The liver can produce glucose through gluconeogenesis and glycogenolysis of stored glycogen, and synthesize cholesterol and triglycerides through lipogenesis. Very low density lipoproteins (VLDL) are synthesized in the liver and loaded with triglycerides and cholesterol to be transported to peripheral tissues. In the insulin resistant state the normal action of insulin on glucose production (Seppala-Lindroos *et al*. 2002) as well as VLDL secretion are impaired (Adiels *et al*. 2007).

Obesity and metabolic syndrome are also associated with Non-alcoholic fatty liver disease (NAFLD), which is characterized by large lipid droplets accumulating inside hepatocytes. NAFLD is usually diagnosed when the liver contains >5% fat of wet weight (Angulo 2002), while excluding fatty liver from other known causes such as viral infections and excess alcohol consumption. The content of liver fat in NAFLD is closely associated with measures of hepatic insulin resistance (Seppala-Lindroos *et al*. 2002). NAFLD may progress from simple steatosis to Non-alcoholic steatohepatitis (NASH) and cirrhosis (Angulo 2002). The accumulation of liver fat is a result of the imbalance in FFA inflow and de-novo-lipogenesis in liver outweighing VLDL triglyceride excretion and beta-oxidation (Lewis *et al*. 2002, Postic *et al*. 2008).

2.4.3 Fatty acid composition of body fat

In the 50’s animal and human studies indicated that dietary unsaturated fat could have a beneficial impact on serum cholesterol levels, which is an indicator of CVD risk. This sparked an interest in dietary studies with the intent of determining the optimal composition of dietary fat for lowering serum cholesterol. Studies on dietary habits proved difficult, due to the propensity of underestimating food intake in obesity (Lichtman *et al*. 1992). As adipose tissue stores excess energy as triglycerides, interest turned to the adipose tissue fatty acid composition as a potential surrogate marker of dietary fat composition.

Controlled feeding trials in humans indicated that the content of linoleic acid (18:2n-6) in adipose tissue began to resemble the linoleic acid content of the long term diet (Seidelin 1995). In contrast, the individual saturated and monounsaturated fatty acids have not been found to be good markers of their dietary intake, likely a result of these being readily synthesized and interconverted in the body. Adipose tissue *trans* fatty acids have also been found to accurately reflect the profile of common dietary *trans* fatty acids (Hudgins *et al*. 1991). Overall, adipose tissue fatty acid composition could only explain a small fraction of the variance in plasma cholesterol levels (Berry *et al*. 1986).

Adipose tissue ω-3 PUFA content has also been found to be related to dietary intake. However, there seems to be a preference in the uptake of ω-3 PUFA with 22 carbon atoms, namely docosapentaenoic acid (22:5n-3) and docosahexaenoic acid (22:6n-3) (Seidelin 1995). Adipose tissue long chain ω-3 PUFA have also been observed to increase with age, independent of dietary intake (Bolton-Smith *et al*. 1997).

Data on the fatty acid composition of liver fat is scarce as obtaining liver biopsies for analysis is an invasive procedure associated with morbidity and mortality. Two studies have, however, reported decreased long chain PUFA in the triglycerides of subjects with NAFLD compared to healthy controls (Araya *et al*. 2004, Puri *et al*. 2007).

2.4.4 Impact of dietary intake on liver fat

As excess caloric intake drives obesity there has been much interest in determining the independent effects of different dietary components on insulin resistance and liver fat.

Increasing saturated fat intake at the expense of monounsaturated fat has been shown to impair insulin sensitivity (Vessby *et al*. 2001). Also, isocaloric diets showed that a high fat diet increased liver fat compared to a low fat diet (Westerbacka *et al*. 2005). *Trans* fat intake, as studied by self reported intake, has been found to increase waist circumference (Koh-Banerjee *et al*. 2003) and obesity (Field *et al*. 2007). More recent studies have identified dietary fructose as promoting insulin resistance (Stanhope *et al*. 2009) and ectopic fat deposition (Le *et al*. 2009). Interventional studies have also indicated that liver fat is increased by excess energy intake, with saturated fat, *trans* fat, and fructose considered more harmful dietary constituents (Sullivan 2010). A 2g/day ω-3 supplementation for six months improved NAFLD (Spadaro *et al*. 2008), although an earlier study with 3.6g/day ω-3 supplementation for three months did not affect insulin sensitivity (Vessby *et al*. 2001). Hypocaloric diets seem to be most effective at lowering liver fat content and improving insulin sensitivity (Sullivan 2010).

3 Aims of the study

Specific aims of the thesis are:

1. To determine the feasibility of using FTIR-ATR for the mid-infrared spectrum of adipose tissue triglycerides. (Study I)

2. To resolve the underlying components contributing to the *trans* and *cis* double bond regions of the mid-infrared spectrum by multivariate curve resolution. (Study I)

3. To measure the echo time behaviour of the four main triglyceride resonances (olefinic, diallylic, methylene, and methyl) in oils with a range of known fatty acid compositions on a clinical MR imager. (Study II)

4. To study the feasibility and usefulness of a long echo time ^{1}H-MRS protocol for measuring adipose tissue fat composition *in vivo*. (Studies II and III)

5. To compare the performance of the long echo time ^{1}H-MRS *in vivo* protocol with gas chromatographic analysis in measuring adipose tissue fat composition. (Study III)

6. To extend the long echo time ^{1}H-MRS protocol to measuring the composition of liver fat *in vivo*. (Study IV)

7. To determine the unsaturation of liver fat relative to subcutaneous and visceral adipose tissue. (Study IV)

4 Materials and methods

Table 1 *Materials and methods used in each study.*

Study	**I**	**II**	**III**	**IV**
Materials				
Oil phantoms		X		X
Pure triglycerides	X			
Healthy volunteers		X	X	
Obese subjects	X			
MetS subjects				X
Methods				
FTIR (*in vitro*)	X			
^{1}H-MRS of adipose tissue		X	X	X
^{1}H-MRS of liver				X
Adipose tissue biopsies	X		X	
Gas Chromatography		X	X	
^{1}H-NMR (*in vitro*)	X[a]	X[b]		

a with a 9.4 Tesla magnet, *b* with a 11.7 Tesla magnet

4.1 Phantoms and Subjects

4.1.1 Oils and pure triglycerides (I and II)

Ten edible oils with a wide range in fatty acid compositions were chosen as phantom material: cod liver, olive, linseed, rapeseed, sunflower, frying, pumpkin, peanut, sesame and walnut oil. Fat could not be used as phantom material due to hardening at room temperature, which will affect the observed T_2-relaxation. Oils were also chosen specifically for the ^{1}H-MRS measurements as the minimum VOI size of 1 cm^3 in single voxel spectroscopy is not practical for measuring expensive pure triglyceride samples.

For FTIR studies, where much smaller samples can be measured, pure triglycerides were used as standards. The four pure triacylglycerol (SigmaAldrich) standards were; Tristearin (stearic acid, 98% grade purity), Triolein (oleic acid, 99% grade purity) and Trilinolein (linoleic acid, 98% grade purity), Trilinolenin (linolenic acid, 98% grade purity). Tristearin was, however, found to exhibit spectra uncharacteristic to triglycerides due to its crystalline structure.

4.1.2 Adipose tissue biopsies (I and III)

For *in vitro* studies adipose tissue biopsies were obtained from abdominal subcutaneous adipose tissue by the needle aspiration technique under local anaesthesia. Study I included biopsies from 16 subjects (11F) and study III included biopsies from 10 subjects (4F). To prevent sample degradation, biopsy samples were immediately placed in liquid nitrogen and stored in a refrigerator at -70 °C.

4.1.3 Obese subjects (I)

Adipose tissue samples used for FTIR studies originated from 16 (11F) massively obese patients (BMI > 41) scheduled to undergo a gastric banding operation.

4.1.4 Subjects with metabolic syndrome (IV)

In order to study the composition of liver fat in non-alcoholic fatty liver disease (NAFLD), 16 subjects (3F) were recruited for ^{1}H-MRS measurements. Thirteen of the subjects had metabolic syndrome according International Diabetes Federation criteria (Alberti *et al*. 2005). Subjects with excessive alcohol intake (>20g per day for males and >10g per day for and females) were excluded.

4.1.5 Healthy volunteers (II and III)

Healthy lean (BMI < 30) volunteers with no contraindications for MRI were recruited for ^{1}H-MRS measurements, with ten subjects also undergoing adipose tissue biopsy studies. Study II included five volunteers and Study III included 17 volunteers.

4.1.6 Blood analysis (I, III and IV)

For all subjects blood samples were obtained after an overnight fast. Samples were used to analyze glucose, insulin, total cholesterol, low-density lipoprotein (LDL), high-density lipoprotein (HDL) and triglyceride concentrations.

4.2 FTIR measurements (I)

All infrared spectra were measured on a Nicolet Nexus 8700 FT-IR spectrometer (ThermoNicolet Analytical Instruments, Madison, WI) equipped with an attenuated total reflectance (ATR) accessory and a Deuterated Triglycine Sulfate (DTGS) detector. As atmospheric H_2O and CO_2 have high intensity mid-infrared absorbances, the spectrometer

was continuously purged with dry nitrogen. The spectra were acquired with 64 scans at 8 cm^{-1} resolution, as this provided adequate signal-to-noise at reasonable measurement times (approx. 1 minute). Between measurements, the ATR crystal was scrubbed with ethanol and a 100% transmission line was measured to ensure the crystal was clean.

For adipose tissue samples, a small lipid droplet was pressed with tweezers upon the ATR crystal. The mid-infrared spectrum of the lipid droplet was subsequently measured and simultaneously monitored for presence of non-triglyceride tissue structures. Tissue water, carbohydrates, and proteins have characteristic absorbances at wavelengths, 1500-1600 cm^{-1} and 3200-3800 cm^{-1}, absent of triglyceride absorbances. Absorbances at these wavelengths indicated contamination by non-triglyceride species and resulted in repetition of the measurements. All measurements were repeated until a pure triglyceride spectrum was observed.

4.3 ^{1}H-MRS measurements (II, III and IV)

^{1}H-MRS measurements were performed on a clinical 1.5 Tesla MR Imager “Avanto” (Siemens, Erlangen, Germany). PRESS was used for acquisition and a combination of a flex-coil and spin-coils were used for signal reception. For MR images the body coil was used for receiving the signal.

Ten oils were measured at room temperature (20 ˚C) and five oils also measured in warm water baths (35 ˚C) to determine the effect of physiological temperatures on echo time behaviour.

For subcutaneous adipose tissue measurements the PRESS VOI was localized in the right dorsal waist region avoiding skeletal muscle, and for measurement of visceral adipose tissue in the right intra/retroperitoneal region avoiding kidneys and intestines. In the liver, the PRESS VOI was localized in the right liver lobe avoiding large veins and bile ducts. For the measurements, the flex coil was positioned over the organ of interest perpendicular to the main magnetic field to maximize sensitivity.

All spectra were acquired with 1024 data points over a 1000 Hz bandwidth, with no water suppression. Pre-processing steps, including shimming and frequency determination, were performed automatically by the imager. In the oils, TR of 1500 ms, in adipose tissue TR of 3000 ms, and in liver TR > 3000 ms (due to respiratory triggering) were used. To examine the echo time behaviour, a range of echo times were acquired for each sample. In the oils TE was 30, 50, 80, 100, 120, 140, 160, 180, 200, 220, 240, 260, 280, 300 ms, with acquisitions increasing from 16 to 64 with increasing TE. In humans, TE was 30, 50, 80, 135, 200 ms, acquisitions increasing from 16 to 32 with increasing TE. Additional echo times were sampled specifically for detecting the ω-3 methyl signal, TE = 470 and 540 ms with 96 acquisitions in human adipose tissue and TE = 135, 270, 405, 540, 675 ms with 128 acquisitions in oils. The VOI ranged 8 to 27 ml in volume and was kept cube shaped for all measurements.

In the liver the acquisition of the PRESS signal was triggered to the expiration stage of respiration. Respiratory motion was monitored with a standard air cushion sensor

(Siemens, Erlangen, Germany) placed over the diaphragm. The minimum TR was set at 3000 ms but in practice TR ranged 4 to 8 s, due to varying respiratory cycles.

4.4 Gas chromatography (II and III)

In order to validate the ^{1}H-MRS results, the detailed fatty acid composition of the oils (II) and adipose tissue samples (III) was determined by gas chromatography. Samples were homogenized in 2ml (v/v) chloroform/methanol with 100 mg/l butylated hydroxytoluene. After Folch extraction, fatty acid methyl esters (FAME) were prepared as in (Evans *et al*. 2002) without separation of lipid classes. An Agilent 5890 GC (Agilent Technologies UK) equipped with a 30 m Rtx®-Wax capillary column with 0.53 mm ID and 1 µm film thickness (Thames Restek, Saunderton, UK) was used to determine fatty acid composition with fatty acid identification by commercial lipid standards (SIGMA Aldrich, Gillingham, UK). The detailed fatty acid composition was also converted to proportions of olefinic, diallylic, methylene, and methyl protons, for comparison with ^{1}H-MRS data.

4.5 *In vitro* ^{1}H-NMR of adipose tissue and oils (I and II)

High-field *in vitro* ^{1}H-NMR spectroscopy at 11.7 Tesla was used to analyse the detailed lineshape of triglyceride resonance (II) and at 9.4 Tesla to validate FTIR studies (I).

Eight adipose tissue samples were divided for measurement by ^{1}H-NMR spectroscopy, as well as FTIR, with samples (40 – 200 mg) washed with saline, homogenized in 1 ml of deuterochloroform and centrifuged for lipid extraction. The chemical shifts were referenced to tetramethylsilane (TMS). A Bruker AVANCE 500 DRX spectrometer (Bruker, Karlsruhe, Germany) operating at 9.4 Tesla was used to acquire ^{1}H-NMR spectra at a temperature of 295K. The used protocol had a spectral width of 5300 Hz, 12.4 s acquisition time, 47.6 s relaxation delay, and 32 scans. Spectra were processed and analyzed with NMR software (PERCH Solutions Ltd., Kuopio, Finland) with quantification of different lipids was performed with total-line-shape fitting (Laatikainen *et al*. 1996). The relative fatty acid composition of the resulting lipid spectra were calculated according to (Willker *et al*. 1998) (Oostendorp *et al*. 2006).

For detailed analysis of oil triglyceride resonance lineshapes at TE = 0 ms and J-couplings, oil samples (30 µl) were dissolved in (650 µl) deuterated chloroform and ^{1}H-NMR spectra at 300K were acquired using Varian Unity Inova 500 spectrometer (Varian Inc., Palo Alto, USA) operating at 11.7 Tesla. The spectral width was 8000 Hz, acquisition time was 2s, relaxation delay was 8 s, and the number of scans was 8. Oil ^{1}H-NMR spectra were analysed by traditional peak integration for the eight distinct fatty acid resonances and three glycerol resonances. For three representative oils (olive, linseed and sunflower), two-dimensional, magnitude-mode COSY spectra were also acquired and used for peak assignment. COSY spectra were recorded with Varian Unity Inova 500 spectrometer at 300K using spectral width of 4473 Hz, 1342 complex data points, 350

number of increments, and 2 repetitions. The data was apodized using a sine function and the final data matrix after Fourier transform was 1024x1024 complex data points.

4.6 Analysis of infrared spectra by MCR (I)

All infrared spectra were analyzed with the Unscrambler v9.6, a software designed for multivariate analysis of chemical data. Multivariate curve resolution was chosen for analysis as it can decompose mixture spectra into components of pure spectra and concentrations to be used for chemical analysis. The Unscrambler uses an alternating least squares (ALS) algorithm to iteratively solve equation 3, which enables the use of multiple constraints. Two spectral regions containing *cis* double bond (2989-3032 cm^{-1}) and *trans* double bond (929-995 cm^{-1}) absorbances were chosen for further analysis by MCR. In order to evaluate the repeatability of the combined FTIR-MCR method, a set of adipose triglyceride spectra were re-measured and analysed by MCR.

4.6.1 MCR of the *cis*-region (I)

The *cis*-region contains absorbances from MUFA and PUFA double bonds with the exact absorption wavelength determined by the number of double bonds in the fatty acid chain (Yoshida *et al*. 2004), ranging 3005-3012 cm^{-1} in natural fatty acids. The wavelength differences are too narrow for resolving different fatty acids, and consequently a single *cis* double bond absorbance is observed in natural triglyceride mixtures. The ability of MCR to resolve the contributions of different fatty acid to the *cis*-region was tested with different data sets, and with and without the use of initial estimate. The *cis*-region of measured of pure triglyceride spectra (triolein, trilinolein, and trilinolenin) were used as initial estimates.

4.6.2 MCR of the *trans*-region (I)

The *trans*-region contains absorbances from isolated *trans* double bonds (at 966 cm^{-1}) (Fritsche *et al*. 1998), conjugated *cis*-*trans* double bonds (at 948 cm^{-1} and 984 cm^{-1}) (Christy *et al*. 2003), and an absorbance at 956 cm^{-1} assigned to saturated fat (Mossoba *et al*. 2007). These absorbances were not resolved in spectra of human triglycerides. The ability of MCR to resolve these resonances and provide a bias free estimate of the isolated *trans* double bond absorbance was tested with multiple data sets. No pure spectra of *trans*, conjugated linoleic acid (CLA) or saturated fat were available for use as an initial estimate for the MCR analysis.

4.7 Analysis of ^{1}H-MR spectra (II, III and IV)

All ^{1}H-MR spectra measured at 1.5 Tesla were analyzed by jMRUI v3.0 software specifically developed for analysing *in vivo* MR spectra. Information obtained from *in vitro* ^{1}H-NMR spectra of oils at 11.7 and 1.5 Tesla served as prior knowledge for subsequent analysis of 1.5 Tesla *in vivo* measurements of fat. All spectra were zero filled to 4096 data points and phased to pure absorption spectra. Peak areas were determined by AMARES, with all spectra and lineshapes set to zero phase (first and second order) and the chemical shift scale fixed to the methylene resonance at 1.3 ppm.

4.7.1 Analysis of echo time series (II)

For analysing the echo time behaviour of the four well resolved triglyceride resonances, each resonance was first isolated by filtering out the unwanted resonances with a Hankel-Lanczos filter (single variable decomposition method) (Pijnappel *et al*. 1992). This provided four sets of spectra containing only the echo time series of olefinic, diallylic, methylene, and methyl resonances. The echo time series of the resonances were determined by fitting a single Lorentzian lineshape to the resonance. This was done to simplify the analysis of a large data set of complex spectra, and to better predict the behaviour for *in vivo* signals displaying limited homogeneity. The performance of the Hankel-Lanczos filter is illustrated in Figure 3.

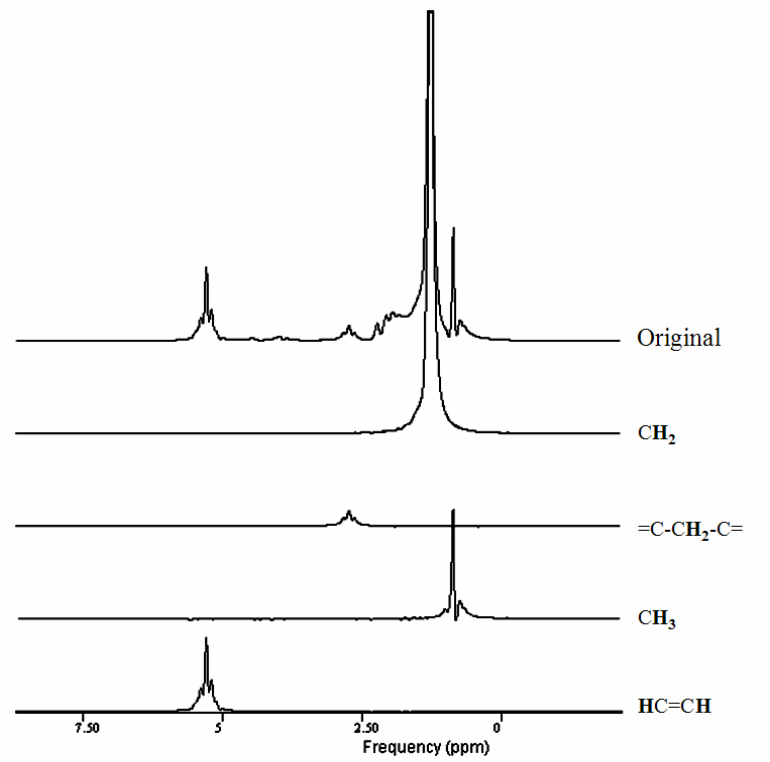

Figure 3 *Separation of the four main resonances (CH_2, =C-CH_2-C=, CH_3, and HC=CH) by a Hankel-Lanczos filter, in Peanut oil at TE = 50 ms.*

4.7.2 AMARES of short and long TE triglyceride spectra (II and III)

For complete analysis of short and long echo time spectra, all resonances were included in the AMARES fit. As the *in vivo* lineshapes do not conform to pure Lorentzian or Gaussian singlets, multiple lineshapes were used for individual resonances. In short TE oil and adipose tissue spectra the olefinic (HC=CH at 5.3 ppm), diallylic (=C-CH_2-C= at 2.8 ppm), and methyl (CH_3 at 0.9 ppm) resonances resembled convolved triplets and were fitted with three Gaussian lineshapes. At long TE, J-modulation of these resonances resulted in singlet like structure and consequently a single Gaussian lineshape was used. Two lineshapes were used for the relatively intense methylene (CH_2 at 1.3 ppm) resonance, one Gaussian and one Lorentzian, at all echo times. The alpha carbon (CO-CH_2-C) and allylic (C-CH_2-C=C) resonances were fitted with Gaussian singlets, but could not be resolved and were therefore not used as markers of FA composition. In adipose tissue spectra, the relatively low intensity water (H_2O at 4.7 ppm) resonance was fitted with a Gaussian singlet. Resonance frequencies were not fixed but constrained to narrow intervals, as FA resonances may exhibit slight shifts in resonance frequencies (Guillén *et al*. 2003).

4.7.3 AMARES of the ω-3 methyl peaks (II and III)

In oils the methyl region was analyzed separately for determining differences between ω-3 and non-ω-3 methyl resonance behavior. High-ω-3 oils were found to display four distinct methyl peaks as opposed to only one in non-ω-3 oils. The three additional peaks for ω-3 corresponded to the ω-3 methyl triplet with peak positions at 1.08, 0.97, and 0.84 ppm. Phase behavior of the left outer triplet line at 1.08 ppm was estimated by fitting a Lorentzian lineshape without phase constraints in AMARES. For estimating ω-3 methyl T_2-relaxation from in-phase spectra, all four methyl peaks were fitted with Gaussian lineshapes fixed to 1.08, 0.97, 0.90, and 0.84 ppm.

For AMARES fitting of *in vivo* adipose tissue spectra (TE = 540 ms), the ω-3 methyl peaks at 1.08 ppm and 0.97 ppm were fitted with Gaussian lineshapes with fixed frequency, and fixed relative amplitude and linewidth. The methylene and non-ω-3 methyl resonances were both fitted with two lineshapes, one Gaussian and one Lorentzian.

4.7.4 AMARES of Liver fat (IV)

Compared to adipose tissue spectra, liver spectra are plagued by broader linewidths and a lower signal-to-noise ratio due to liver motion and tissue inhomogeneity. Also the high intensity H2O resonance in liver may interfere with proper fitting. Therefore, in AMARES fitting of liver spectra, a more robust approach was used. A single Gaussian was used for all lipid resonances, with relative frequencies and linewidths fixed to those estimated from the methylene resonance. Liver tissue water was fitted with two lineshapes, one Gaussian

and one Lorentzian, which improved fitting accuracy. When comparing liver fat composition to adipose tissue fat composition, identical AMARES fits were used.

4.7.4 Calculation of fat composition and T_2-relaxation (II, III and IV)

Indices of fat composition were calculated as olefinic/methylene, diallylic/methylene, and methylene/methyl ratios. Also the ω-3 methyl resonance (sum of peaks 1.08 and 0.97 ppm) was divided with the methylene peak. A monoexponential fit was used to estimate T_2-relaxation of methylene and water resonances.

To be able to relate the long TE ^{1}H-MRS data to previously published GC data, the olefinic proton content derived from TE = 200 ms spectra was converted to the number of double bonds per FA chain (DB/FA). For data conversion a simple linear regression model was constructed with data obtained from five oil phantoms. The calibration model ($\mathbf{Y} = b\mathbf{X} + a$) related the olefinic proton content measured at TE = 200 ms ($\mathbf{X}$) to the number of double bonds per FA chain determined by GC ($\mathbf{Y}$). The correlation coefficient ($R = 0.998$) and standard error of estimate (0.014) indicate the model performed well.

5 Results

5.1 Subject characteristics (I, III and IV)

Subject characteristics in studies I, III and, IV, table 2. Two of the obese subjects in study I had been diagnosed with T2D.

Table 2 *Characteristics of study subjects. Data presented as mean ± standard deviation.*

	Study I	**Study III**	**Study IV**
Characteristic			
Gender	5M/11F	9M/8F	13M/3F
Age (y)	44±9	46±13	55±8
Weight (kg)	149±31	78±9	94±14
BMI (kg/m^2)	52±8	25±4	32±4
Waist (cm)	148±17	89±8	108±10
P-Glucose (mmol/l)	6,7±2,4	5,3±0,7	5,7±0,6
S-Insulin (mU/l)	30,1±26,9	-	13,9±6,7
S-TG (mmol/l)	1,9±0,54	1,3±0,6	2,2±1,1
S-Total cholesterol (mmol/l)	5,6±1,1	4,7±1,0	5,1±0,8
S-HDL-cholesterol (mmol/l)	1,1±0,2	1,6±0,6	1,0±0,2
S-LDL-cholesterol (mmol/l)	-	2,5±1,3	3,2±0,6

5.2 Infrared spectroscopy and MCR of adipose tissue lipid droplets (I)

Manually pressing a lipid droplet onto the ATR crystal resulted in a pure triglyceride spectrum absent of vibrations from other tissue structures, Figure 4. The triglyceride spectrum showed peaks characteristic to triglyceride composition previously described by studies on oils and animal fat. A characteristic adipose tissue triglyceride spectrum is shown in Figure 4 with the *trans*- (A) and *cis*-double bond (B) regions labelled. Good coverage of the ATR crystal was obtained as shown by the small variance in the intensity of the triacylglyceride ester carbonyl stretch at 1744 cm^{-1}. Contamination by non-TG adipose tissue structures could be observed by vibrations in the O-H and N-H region around 3100 – 3600 cm^{-1}, absent in pure TG spectra (Guillen *et al*. 1997).

The MCR algorithm showed that two pure components could be resolved in the olefinic region with peak positions at 3005 cm^{-1} and 3010 cm^{-1}. The peak at 3005 cm^{-1} was assigned to MUFA =C-H (-*cis*) stretching vibrations and the peak 3010 cm^{-1} to PUFA =C-H (-*cis*) stretching vibrations. The MUFA peak is known to appear at this charcteristic frequency (Yoshida *et al*. 2004), which was also confirmed by the peak position of the

=C-H (-*cis*) stretch in pure triolein. The individual PUFA also exhibit characteristic frequencies determined by the amount of double bonds in the fatty acid chain ranging from 3009 cm^{-1} for linoleic acid (18:2n-6) to 3012 cm^{-1} for arachidonic acid (20:4n-6) (Yoshida *et al*. 2004), also confirmed by our measurements on pure triglycerides. The PUFA peak resolved by MCR in the olefinic region appeared at 3010 cm^{-1}, thus representing total adipose tissue PUFA double bonds. Further attempts at resolving the individual fatty acids of the PUFA peak did not produce reproducible results, probably due to insufficient signal-to-noise. Also, PCA showed that two principal components accounted for 99.1% of the variance in the data, indicating no further information beyond two components could be extracted. When performing MCR without pure TG spectra as an initial guess, the peak positions of the two resolved peaks migrated closer to each other away from the characteristic MUFA and PUFA frequencies.

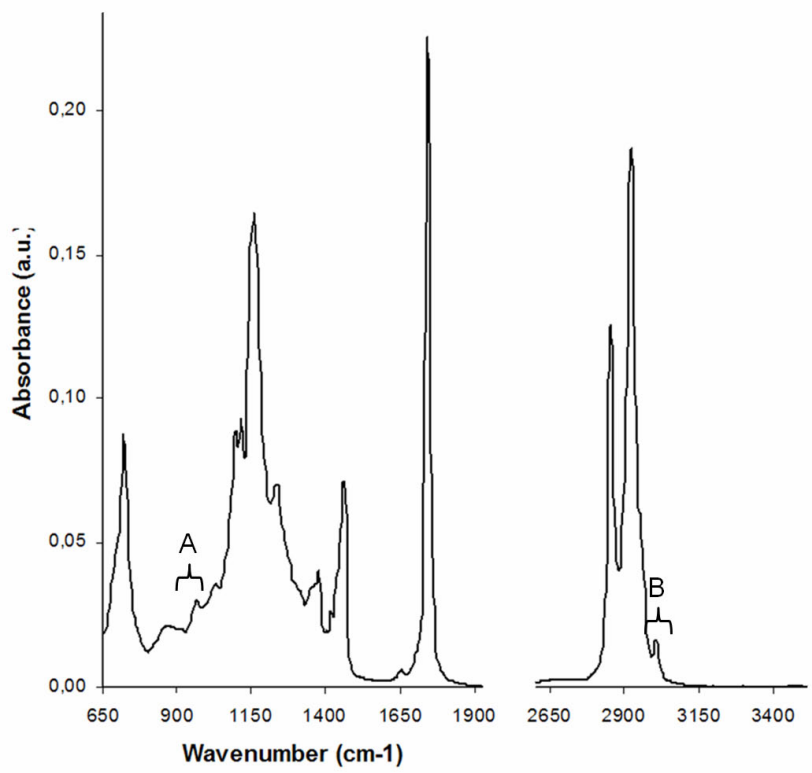

Figure 4 *Mid-infrared spectrum of a lipid droplet pressed from human adipose tissue. The regions used for MCR analysis are labelled, (A) trans region and (B) cis region.*

Using MCR on the *trans* region resolved three pure components with PCA indicating three principal components accounted for 98.5% of the underlying variance. The three components were assigned isolated *trans* isomers at 966 cm^{-1}, conjugated linoleic acids (CLA) at 948 cm^{-1} and 984 cm^{-1} (Fritsche *et al*. 1998, Christy *et al*. 2003) and a broad background vibration arising from saturated fatty acids at 956 cm^{-1} (Mossoba *et al*. 2007). No initial guess was used for MCR of the *trans* region as the results were reproducible as such. Measured spectra and MCR resolved pure components of the olefinic and *trans* regions are shown in Figures 5 and 6.

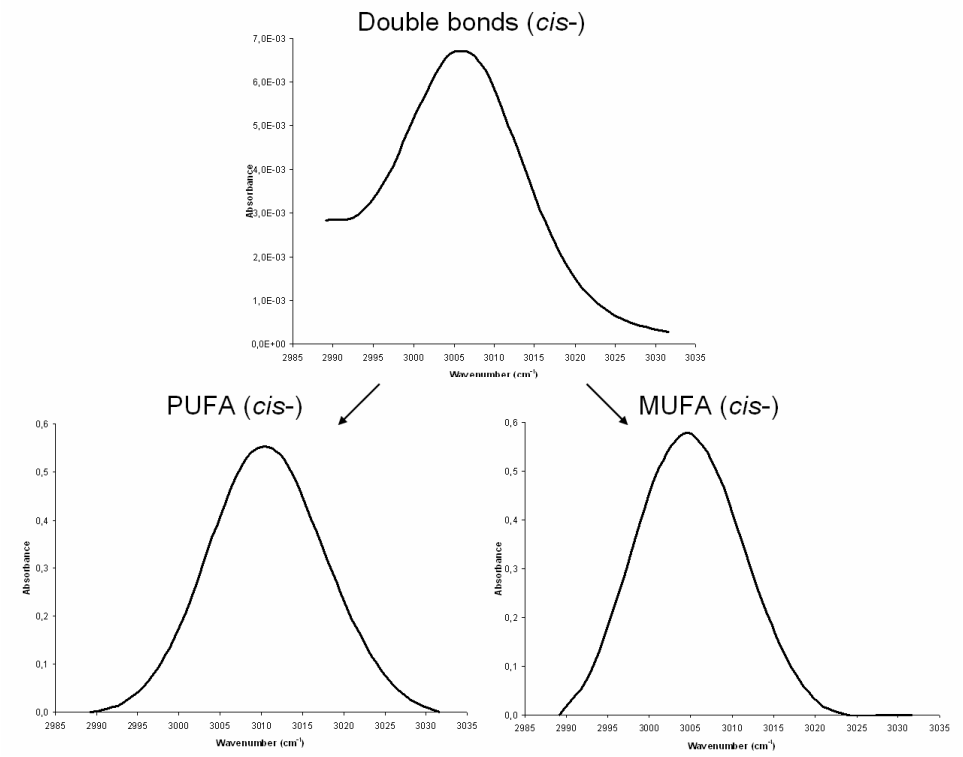

Figure 5 *MCR analysis of the cis- region. Two components were resolved in the cis region, PUFA and MUFA double bonds.*

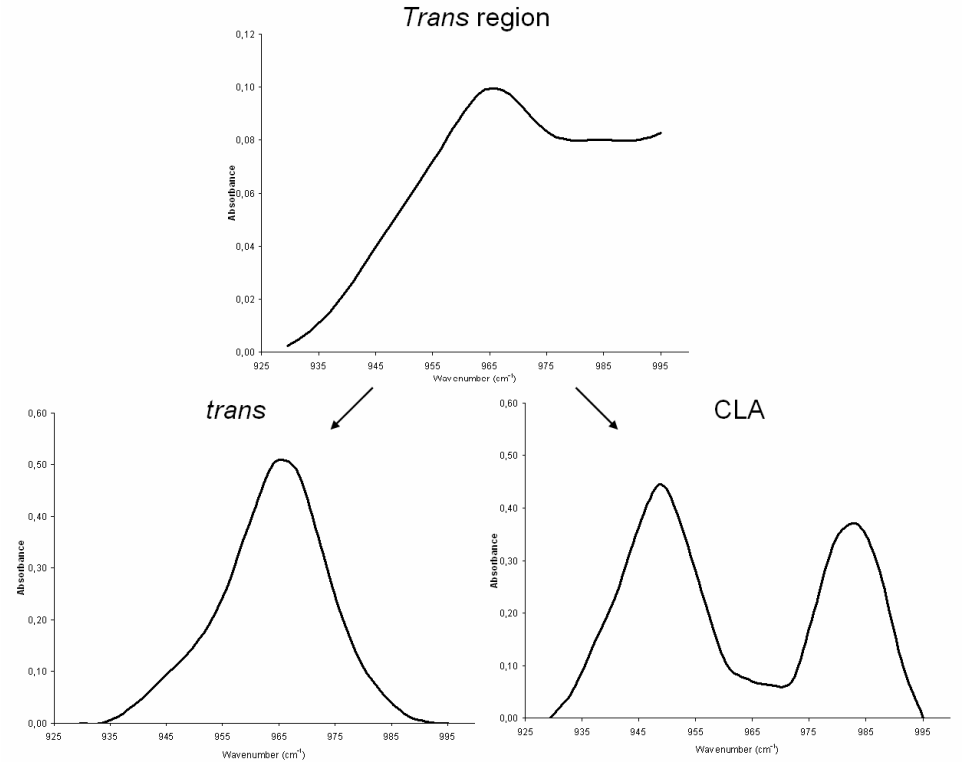

Figure 6 *MCR analysis of the trans region. Three components were resolved in the trans region with isolated trans isomers and CLA shown.*

The MCR results were repeatable for the MUFA, PUFA and *trans*FA with repeated measures showing correlations R > 0.966 and coefficients of variation < 3.1%. Due to the low concentration of CLA in adipose tissue (Hudgins *et al*. 1991) and a resulting poor signal-to-noise, estimation of CLA content was somewhat unreliable, with R = 0.889 and 30.8% CV for repeated measurements. Validation by ^{1}H-NMR showed positive correlations for MUFA (R = 0.888, P < 0.01) and PUFA (R = 0.918, P < 0.01). The total *cis* double bond peak area estimated by peak integration directly from infrared and ^{1}H-NMR spectra also correlated (R = 0.915, P < 0.01).

5.3 ^{1}H-MRS of oil phantoms (II)

Analysis of the oil phantom echo time series showed very similar response curves for the olefinic, diallylic, and methylene resonances, despite large differences in fatty acid composition. The echo time behaviour of the methyl resonance, however, showed clear dissimilarities between oils high in ω-3 FA (linseed, cod liver, rapeseed, walnut) and low ω-3 FA oils (fry, olive, peanut, pumpkin, sesame, sunflower). The echo time behavior of oils representative of MUFA (olive), PUFA (sunflower), and ω-3 (linseed) are shown in Figures 7 and 8.

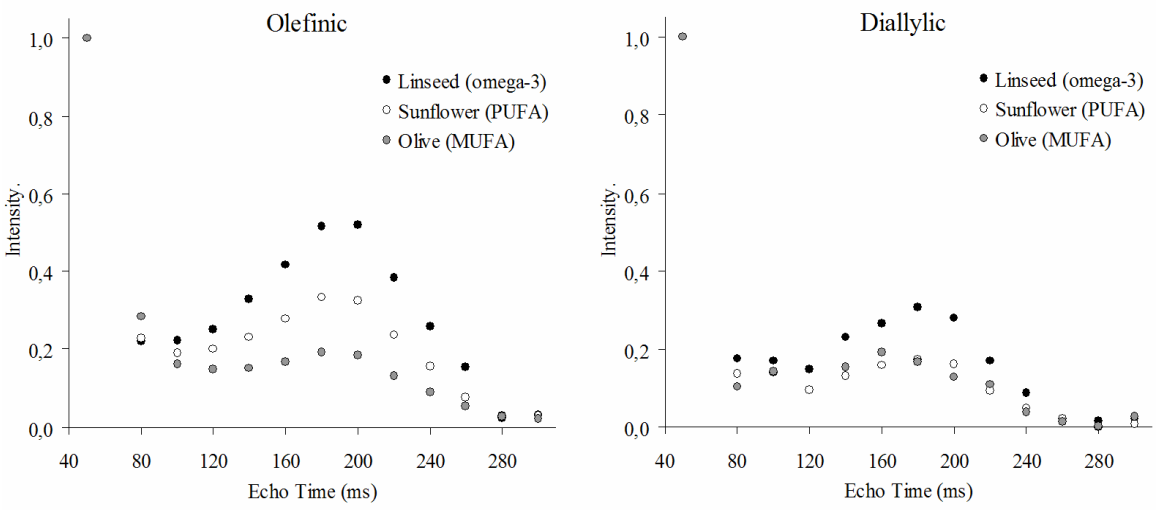

Figure 7 *Echo time behaviour (TE=50-300 ms) of the olefinic and diallylic resonances in representative oils.*

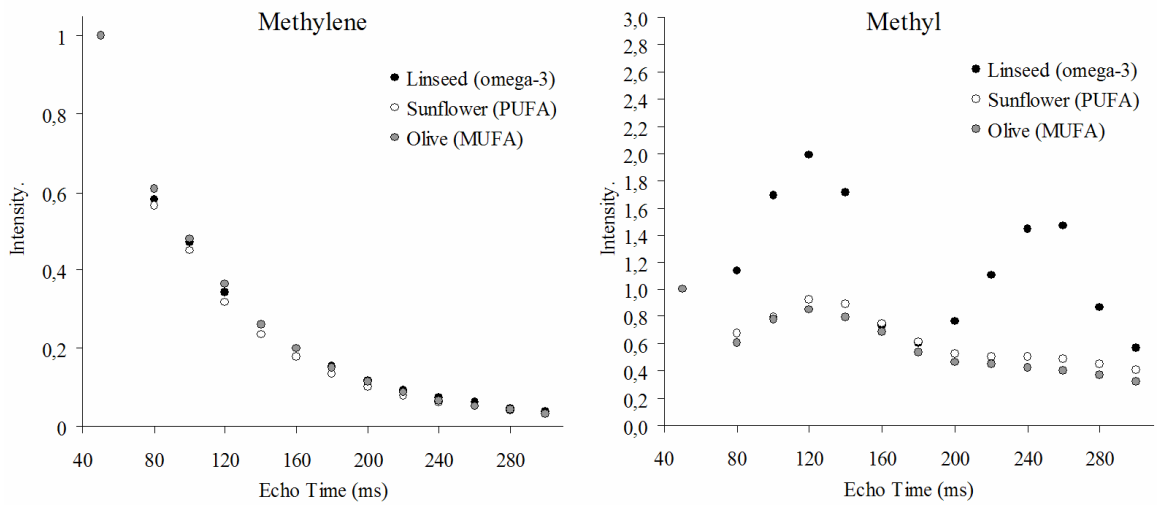

Figure 8 *Echo time behaviour (TE=50-300 ms) of the methylene and methyl resonances in representative oils. All intensities normalized to TE = 50ms.*

The characteristic echo time behaviour of the methyl resonance in oils high in ω-3 FA, was due to the ω-3 methyl resonance showing traditional weak coupling behavior, while non-ω-3 methyl resonance showed strong coupling. This was evident from detailed examination of the spectra. In Figure 9 the characteristic echo time behavior of the methyl resonance in linseed and sunflower oils are shown (TE=70-140ms). The in-phase anti-phase behavior of the ω-3 methyl outer triplet lines is clearly visible while sunflower oil (mainly ω-6 PUFA) shows a singlet like structure. Two-dimensional COSY spectra of linseed oil indicated methyl protons at 0.9 ppm coupling with allylic protons at 2.0 ppm, while in sunflower oil spectra the methyl resonances at 0.9 ppm only coupled to methylene protons at 1.3 ppm.

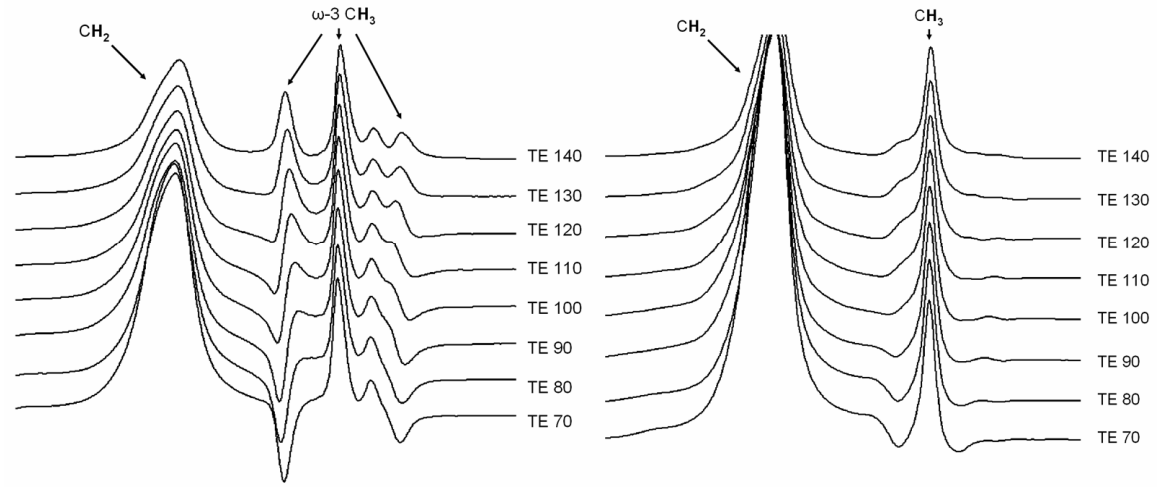

Figure 9 *Methyl region (1.8-0.0 ppm) echo time behaviour TE = 70-140ms, for linseed oil (left) and sunflower oil (right).*

With the implied benefits of long TE for *in vivo* ^{1}H-MRS of lipids, the use of long TE in estimating oil unsaturation was evaluated by comparing the olefinic and diallylic proton contents of oils determined by GC and long TE ^{1}H-MRS (TE = 200 ms). Both measures of oil composition showed good correlations between the two methods, although long TE ^{1}H-MRS overestimated the olefinic proton content, see Figure 10.

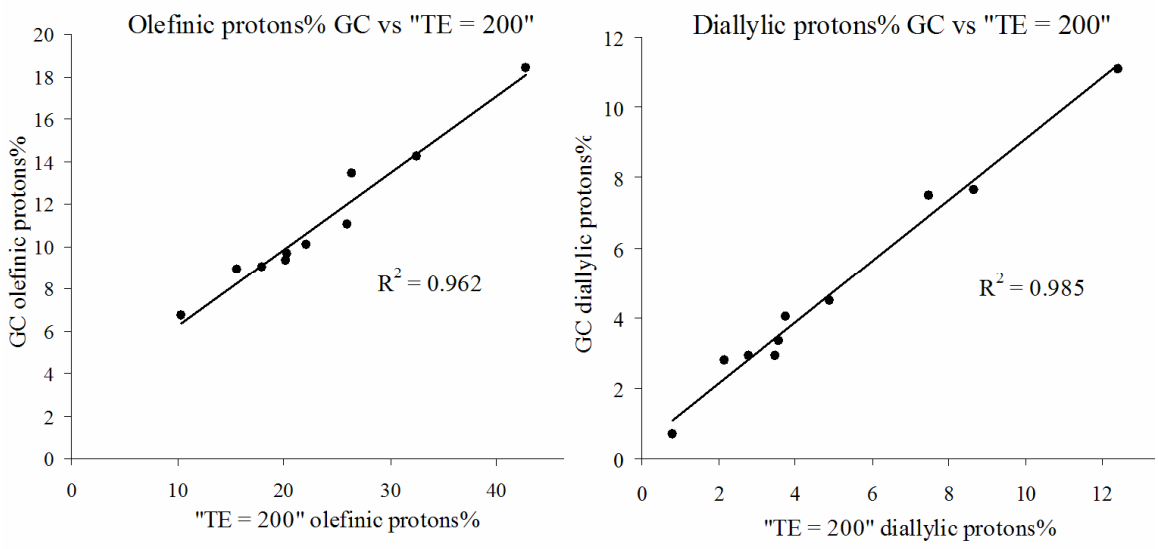

Figure 10 *Correlation between oil composition determined by GC and long TE ^{1}H-MRS (TE=200ms). Olefinic (left) proton content and diallylic (right) proton content.*

Analysis of the left outer triplet line of the ω-3 methyl group showed an in-phase anti-phase behavior with a period of 135 ms. Determining oil ω-3 FA content by the outer methyl triplet line in TE = 140 ms spectra correlated strongly with ω-3 FA content determined by GC (R = 0.999).

There was no difference between the oil spectra measured at 20 ˚C and 35 ˚C. However, the methylene T_2 increased from 77.6±4.5 to 91.1±3.8 ms, with increasing temperature. The indices of oil composition determined from long TE spectra were not affected by the temperature.

5.3 ^{1}H-MRS of adipose tissue (II and III)

Pilot studies of adipose tissue fat composition indicated that the improved peak separation and baseline characteristics of long TE ^{1}H-MRS resulted in improved fitting accuracy with AMARES. Importantly, also the ω-3 FA methyl peak at 1.08 ppm could be resolved at very long echo times, with characteristic in-phase (TE = 540 ms) anti-phase (TE = 470 ms) behavior.

Using ^{1}H-MRS to characterize adipose tissue fat composition was compared to the detailed fatty acid composition of adipose tissue determined by GC. Increasing echo time

resulted in improved correlations between ^{1}H-MRS derived indices of fat composition and those determined by GC. Specifically, the estimation of diallylic proton content by ^{1}H-MRS improved from a correlation of R = 0.379 (not significant) at TE = 30 ms to R = 0.952 (P < 0.001) at TE = 135 ms to GC determined diallylic proton content. The improved correlation was a result of improved fitting accuracy as shown by the reduced Cramer-Rao lower bounds. A similar trend of improved peak fitting with long echo times was observed for the olefinic proton contents. The methylene-to-methyl ratio of long TE spectra was not related to adipose tissue PUFA content or the GC determined CH_2/CH_3, but correlated negatively with MUFA content with a trend for a positive correlation to SAFA content. The average double bond content of PUFA chains correlated positively with the position of the diallylic peak (R = 0.899, P < 0.001).

In 17 healthy subjects, no correlations between ^{1}H-MRS derived indices of fat composition and serum lipid levels (LDL, HDL, TG) were observed. The diallylic proton content determined from TE = 135 ms spectra showed a positive correlation with age (R = 0.569, P = 0.017, N = 17). The T_2-relaxation time of the methylene resonance indicated minor inter-individual variance (T_2 = 88.1±1.1ms).

5.3 ^{1}H-MRS of Liver fat (IV)

Long TE ^{1}H-MRS at TE = 200 ms was found to be able to resolve the olefinic resonance at 5.3 ppm from the intense liver tissue water resonance 4.7 ppm in subjects with liver fat greater than 5%. The AMARES fitting procedure performed well with the main lipid peaks obtaining CRBs of below 6%. The number of double bonds per fatty acid (DB/FA) in liver fat was 0.812±0.022, which was significantly lower than in subcutaneous (0.862±0.022) and visceral (0.865±0.033) adipose tissue (P < 0.0004). The T_2 of the methylene resonance was found to be significantly shorter in liver (T_2 = 72.4±4.1ms) compared to subcutaneous adipose tissue (T_2 = 82.3±1.2ms).

Also the diallylic resonance could be well resolved by long TE ^{1}H-MRS at TE = 135 ms, with analysis showing no significant difference between the polyunsaturation in liver (0.327±0.098) and in subcutaneous adipose tissue (0.376±0.043). The liver diallylic resonance was, however, detectable in only those seven subjects who had liver fat content greater than 15%.

Despite considerable attenuation at TE = 200 ms, the water resonance was still the most intense resonance in the spectra and remained a potential confounder when fitting the relatively small olefinic resonance. To determine the effect the large water resonance exerted on fat unsaturation derived from long TE spectra, we re-analyzed the subcutaneous adipose tissue spectra with a measured water resonance added at various intensities. The analysis suggested that a added water resonance corresponding to 4% liver fat content would not alter the derived unsaturation, Figure 11.

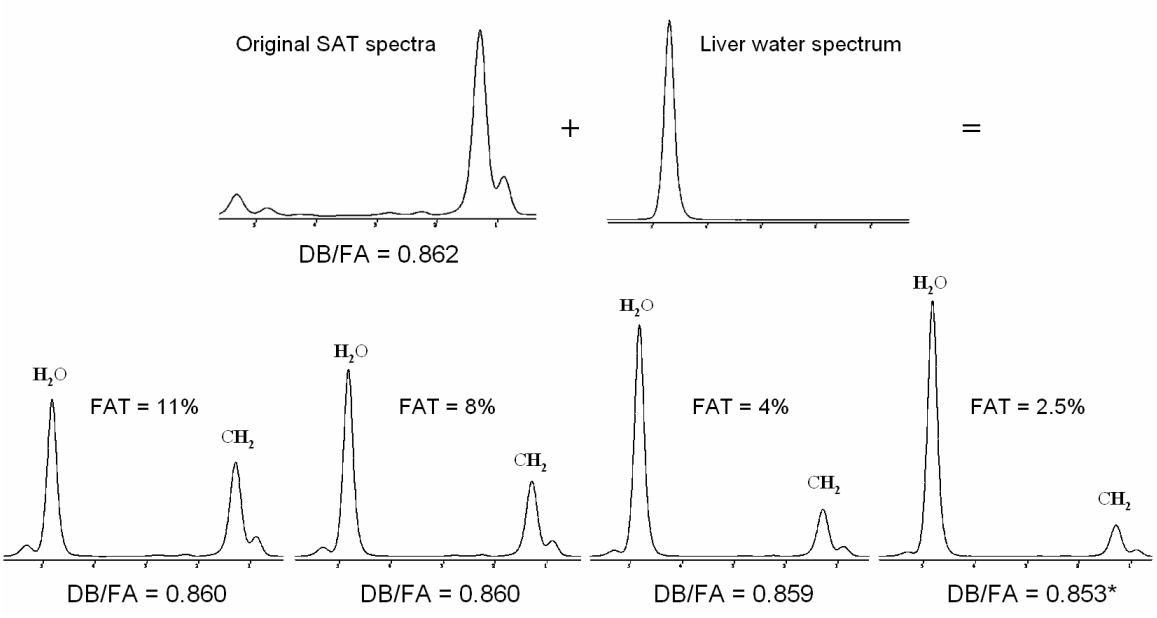

Figure 11 *Water resonance impact on the unsaturation derived from subcutaneous adipose tissue (SAT) long TE spectra. Only in spectra with water content corresponding to 2.5% liver fat, did the unsaturation drop significantly from 0.862 to 0.853, paired t-test (P = 0.03).*

6 Discussion

In this work two different spectroscopic techniques were developed for *in vitro* and *in vivo* analysis of fat composition. Both methods have their advantages and disadvantages compared to traditional gas chromatographic analysis of tissue triglycerides.

6.1 FTIR of adipose tissue triglycerides (I)

Infrared spectroscopy provides a fingerprint of the molecule under study, but most of the arising absorbance peaks cannot be unambiguously assigned to specific fatty acids. An exception is the peak at 966 cm^{-1}, which can be attributed solely to fatty acids containing isolated *trans* isomers (van de Voort *et al*. 2001). However, infrared spectroscopy has advantages; measurements can be performed on neat samples, spectra are well suited for chemometric analysis, and potential to be developed for noninvasive analysis in humans *in vivo*. Also, detecting and quantifying fatty acids with *trans*-isomers is difficult with gas chromatography due to co-elution with *cis*-isomers (Hudgins *et al*. 1991). The ATR accessory has been used to obtain infrared spectra from neat oil and animal fat samples (Guillen *et al*. 1997), but has not been extended to analysis of human adipose tissue.

Traditional peak integration of infrared vibrations is prone to errors arising from peak overlap. The double bond vibration at 3006 cm^{-1} produces a single peak in adipose tissue triglyceride spectra, thus not resolving double bonds from different fatty acids with slight shifts in wavenumber (Yoshida *et al*. 2004). The *trans* region at 966 cm^{-1} has been shown to contain vibrations arising from saturated fatty acids, as well as *trans* and CLA isomers, which can introduce errors when determining triglyceride *trans*FA content at low concentration (< 0.5%) (Mossoba *et al*. 2007). Using Multivariate Curve Resolution (MCR) we were able to resolve spectra of pure components in the olefinic and *trans* regions. The resulting pure spectra are in accordance with what is known of adipose tissue fatty acid composition (Hudgins *et al*. 1991) and fatty acid infrared vibrations in these regions (Fritsche *et al*. 1998, Christy *et al*. 2003) (Mossoba *et al*. 2007). Repeated analysis showed good repeatability, although CLA estimates were influenced by a relatively poor signal-to-noise. Similarly, validating FTIR-MCR with ^{1}H-NMR spectroscopy resulted in reasonable correlations between the two methods.

6.2 Long TE ^{1}H-MRS of fat composition (II, III and IV)

Magnetic resonance spectroscopy is a well established clinical method for obtaining biochemical information noninvasively *in vivo*. The analytical capabilities of *in vivo* ^{1}H-MRS are limited, as the proton spectrum at 1.5 Tesla can only resolve four triglyceride resonances; the olefinic (5.3 ppm), diallylic (2.8 ppm), methylene (1.3 ppm), and methyl resonances (0.9 ppm). Also, broad linewidths, an intense water signal (4.7 ppm), and J-

modulation of the J-coupled lipid protons, are common in *in vivo* conditions leading to peak overlap and poor fitting accuracy. It has been noted that at long echo times triglyceride resonances become better resolved due to J-modulation (Schick *et al*. 1993, Skoch *et al*. 2006). A detailed analysis of the effects of using long echo time for determining fat composition has, however, been lacking.

6.2.1 Oils (II)

Usually pure compounds are used as standards for validating analytical techniques. This can be a problem for *in vivo* ^{1}H-MRS in clinical imagers, since samples exceeding 1 cm^3 are needed. Oils were used in this study as they are inexpensive, represent different fatty acid compositions, and are fluid at room temperature.

Detailed analysis showed that long TE spectra resolved better the four main triglyceride resonances with fatty acid composition having minimal impact on three (olefinic, diallylic, and methylene) of the four resonances. Fatty acid composition also had minimal impact on the apparent T_2-relaxation of the methylene resonance, while increasing temperature to 35˚C significantly increased the apparent T_2 to levels (T_2 = 91 ms) observed in bone marrow fat (T_2 73-90 ms) (Schick 1996) and adipose tissue *in vivo* (T_2 = 91 ms) (studies II and III), indicating temperature has a strong effect on lipid T_2. Long TE indices of unsaturation (olefinic protons) and polyunsaturation (diallylic protons) agreed well with CC data, indicating that long TE might be useful for *in vivo* studies.

6.2.2 GC and ^{1}H-MRS of adipose tissue (III)

Adipose tissue studies confirmed that using long TE improved peak separation and therefore the reliability of the fitting routine, as shown by the improved Cramer-Rao lower bounds. Olefinic and diallylic proton contents derived from long TE spectra also corresponded better with adipose tissue GC data than short TE spectra. A shortcoming of the used AMARES fitting routine was the poor baseline correction.

Several fitting routines can be used for analysis of *in vivo* ^{1}H-MRS lipid spectra, in-house software (Lunati *et al*. 2001), commercial software (LCmodel) (Skoch *et al*. 2006), and the freely available EU-funded software jMRUI (Yeung *et al*. 2005). The AMARES algorithm was chosen for the ability to incorporate prior information and versatile lineshape fitting into the fitting routine (Mierisová *et al*. 1998). Using direct area evaluation (Lunati *et al*. 2001) for *in vivo* spectra can lead to poor results as differences in linewidth cannot be accounted for. The LCmodel software can be used to analyze lipid spectra from muscle and liver, and can correct for an arbitrary baseline, but it has not yet been modified for the analysis of adipose tissue spectra. GC data showed that for the ten healthy subjects, the standard deviation of olefinic and diallylic protons was 4.1% and 12.2%, respectively, while the CH_2/CH_3 ratio had a standard deviation of 0.9%. Considering the commonly used cutoff criterion for acceptable fit is a standard deviation of 20%, normal fitting criteria are not applicable to the study of fat composition.

GC data also indicated that the previously used assumptions for calculating SAFA, MUFA, and PUFA fraction from proton spectra of animal (Strobel *et al*. 2008) and human fat (Ren *et al*. 2008) were unfounded. To calculate the different fatty acid fractions from the proton spectrum it is assumed that all protons contributing to the diallylic resonance arise from linoleic acid (18:2n-6). Although linoleic acid frequently constitutes 90% of all PUFA in human adipose tissue, this does not necessarily hold for the proportion of linoleic acid protons contributing to the diallylic resonance. In our study, the proportion of linoleic acid of all diallylic protons ranged 52 - 78% in adipose tissue, indicating not only a much lower contribution to the diallylic resonance than assumed, but also a fairly high variance. Thus, the previously used assumptions in determining the fatty acid composition from proton spectra will lead to erroneous results, specifically overestimation of the PUFA fraction at the expense of MUFA (Ren *et al*. 2008).

Accurate estimation of fatty acid fractions from proton spectra would, however, be advantageous. The lipid proton spectrum can provide a more accurate analysis of the composition of the diallylic resonance. It is known that the exact resonance frequency of the diallylic resonance of polyunsaturated fatty acids increases with increasing double bond content. For example linoleic acid resonates at 2.78 ppm while docosahexaenoic acid (22:6n-3) resonates at 2.86 ppm (Willker *et al*. 1998). Accordingly, we observed a positive correlation between the resonance frequency of the diallylic signal and the GC determined PUFA double bond content. Using the frequency information to provide a better estimate of the underlying PUFA profile may enable the calculation of fatty acid fractions from the proton spectrum.

6.2.3 ^{1}H-MRS of ω-3 fatty acids (II and III)

Oil studies also revealed differences in the echo time behaviour of the methyl region between oils high or low in ω-3 FA content. The difference was attributed to strong coupling present in non-ω-3 FA where the methyl protons at 0.9 ppm couple to saturated methylene protons at 1.3 ppm ($-CH_2-CH_2-CH_2-CH_3$), while ω-3 FA methyl protons at 0.97 ppm couple to allylic protons at 2.0 ppm ($-HC=CH-CH_2-CH_3$) and exhibit weak coupling. Strong coupling arises when the chemical shift difference (in Hz) between coupled protons is small compared to the coupling constant, which was ~7 Hz for methyl protons as determined from high-resolution ^{1}H-NMR spectra. At 1.5 Tesla with protons resonating at 63.87 MHz, the frequency difference between the methyl and allylic resonances in ω-3 FA is ~66 Hz, while the the frequency difference between the methyl and methylene resonances in non-ω-3 FA is ~26 Hz.

The weak coupling effect seen in ω-3 FA resulted in a methyl triplet, with the outer triplet lines showing in-phase anti-phase behaviour with a period of 135ms with increasing echo time. Using this knowledge, the ω-3 FA left outer triplet line was detected at TE = 540 ms in adipose tissue *in vivo*, making this the first reported non-invasive detection of ω-3 FA in humans *in vivo*. Although more advanced spectroscopic techniques ^{13}C-MRS (Hwang *et al*. 2003), 2D-COSY ^{1}H-MRS (Velan *et al*. 2007), and ^{1}H-MRS at 7 Tesla (Ren *et al*. 2008) have been used to study lipid composition *in vivo*, they have not been reported

to be able to detect ω-3 FA. Unlike 1.5 Tesla ^{1}H-MRS, these more advanced methods are not readily available in clinical imagers.

When comparing human adipose tissue ω-3 FA content determined by long TE ^{1}H-MRS (TE = 540 ms) and GC a positive correlation was observed, indicating that even very long echo times reflect the true ω-3 FA content.

6.2.4 Liver fat composition (IV)

Proton MRS has become the de facto standard for noninvasive quantitation of liver fat content, as it provides, with proper correction factors, a quantitative measure of liver triglyceride wet weight (Szczepaniak *et al*. 2005).

As the liver is not easily sampled in human studies, interest has turned to ^{1}H-MRS as a non-invasive alternative for analysing liver fat composition (Johnson *et al*. 2008). Proton MRS for determining liver fat composition is hampered by broad linewidths, motion artifacts from respiration and pulsation, and overlapping metabolite resonances from H2O, choline, and macromolecules. Johnson *et al*. used ^{1}H-MRS with short TE at 1.5 Tesla to analyze liver fat composition, reporting an increase in saturation with increasing liver fat content (Johnson *et al*. 2008). They obtained good quality spectra by positioning the subject in a right decubitus position on the surface coil, thereby minimizing motion artifacts due to breathing. As was pointed out by Cobbold *et al*., they did, however, erroneously assign the choline resonance (at 3.2 ppm) to diallylic polyunsaturated fat, thereby invalidating the results (Cobbold *et al*. 2008). Johnson *et al*. maintained that the saturation of liver fat increased with increasing liver fat content even when removing the erroneous PUFA peak from the analysis, now relying on the allylic resonance as a measure of saturation (Cobbold *et al*. 2008). Our studies on oils and adipose tissue, however, indicated that the allylic resonance (at 2.0 ppm) is not resolved from the alpha-carbon resonance (at 2.3 ppm) at 1.5 Tesla and should therefore not be used as an indicator of fat composition. Furthermore, when using *in vivo* ^{1}H-MRS to probe fat composition of subjects with a large variance in liver fat content, there is a risk that the observed differences are actually due to differences in the signal-to-noise or the relative contribution from the macromolecule baseline. Johnson *et al*. also used water suppression, which can affect nearby resonances, specifically the olefinic lipid resonance.

By using long TE ^{1}H-MRS with respiratory triggering and without water suppression, we were able to resolve the olefinic resonance at 5.3 ppm from the tissue water resonance at 4.7 ppm and calculate the double bond content of liver fat. The observed DB/FA = 0.812 is in line with GC studies of human liver triglyceride composition in simple steatosis DB/FA = 0.814 (Araya *et al*. 2004). We did not attempt to determine the unsaturation in subjects with liver fat below 5%, as low lipid levels may lead to unreliable results. Further analysis of adipose tissue spectra with added water resonances indicated a liver fat content of 4% was adequate for determining unsaturation from the olefinic resonance.

6.2.5 T_2-relaxation (II, III and IV)

T_2-relaxation effects are a potential error source when using long echo times. Although oil studies indicated that olefinic and diallylic protons coupled to MUFA and PUFA obtain very similar J-modulation curves, the olefinic proton content was overestimated by long TE spectra, indicating potential differences in T_2-relaxation. The correlation between long TE ^{1}H-MRS and GC data for olefinic and diallylic protons was, however, linear in oils as well as in adipose tissue.

All oils also showed similar echo time behaviour for the methylene resonance with minimal J-modulation. This indicates that fatty acid composition has a negligible impact on the methylene decay rate and that the decay rate can be used to probe the T_2-relaxation of triglycerides. The T_2 measured by PRESS should, however, be viewed as an apparent T_2. The methylene protons in fatty acid chains couple predominantly with each other, with a few methylene protons coupling with methyl, allylic and beta-carbonyl protons. These protons have a fairly small chemical shift spread and exhibit complex strong coupling difficult to analyze by ^{1}H-NMR measurements. Analysis of the echo time behaviour of fatty acid resonances by simulations may provide further insight.

The different oils showed only small differences in their T_2 (75.8±3.8ms), with the exception of cod liver oil, which had a fairly long T_2 (85.0ms). This is likely due to greater mobility from the high long-chain ω-3 PUFA content. Adipose tissue T_2 of 91.1±1.2ms, derived from the methylene resonance, accordingly showed very small inter-individual differences. This is in contrast to a previous study indicating an SD of 13.4% in adipose tissue methylene T_2 (Querleux *et al*. 2002), which is likely to arise from poor signal-to-noise from the smaller voxels acquired by STEAM.

Compared to adipose tissue, T_2 (72.4±4.1ms) of liver fat was significantly shorter. This cannot be explained by the higher saturation of liver fat, as even oils with much larger saturation differences did not show considerable differences in T_2. When the liver gradually becomes infiltrated with fat the lipid droplets in liver increase in size. Under the microscope liver lipid droplets range 0-10 µm in diameter (Arola J. personal communication 2010), while adipocyte lipid droplets, which usually encompass the whole cell, are approximately 100 µm in diameter (O'Connell *et al*. 2010). Lipid droplet size is known to affect lipid mobility inside the droplet, as diffusion is restricted in smaller droplets (Lahrech *et al*. 2001, Goudappel *et al*. 2001). We propose that the small lipid droplet size in the liver lead to restricted mobility and therefore a shorter T_2 compared to adipose tissue lipids. Although lipid droplet size has been probed by diffusion NMR, lipid T_2 has not yet been linked to lipid droplet size.

As an isotropic liquid, lipid T_2 relaxation is strongly affected by viscosity, as this affects the dipole-dipole relaxation mechanism through molecular tumbling (Bloembergen *et al*. 1948). The strong increase in lipid T_2 observed when oil temperature was increased can also be attributed to increased lipid fluidity. Despite the strong effect of temperature on T_2, the unsaturation derived from long TE spectra did not change. This can be understood as all resonances attached to the triglyceride molecule experiencing the same induced change in molecular tumbling. As the unsaturation is derived from lipid resonance ratios, macroscopic changes in T_2 of the lipids are effectively cancelled out.

6.3 Tissue differences in fat composition (IV)

Using the novel approach of long TE ^{1}H-MRS, we found that liver fat is more saturated than subcutaneous or visceral adipose tissue, in terms of double bonds per fatty acid (DB/FA). A strong correlation was also observed in the DB/FA between these fat depots, indicating some similarity in the fat composition. Although the DB/FA provides a good general marker of fat composition, it cannot discriminate between SAFA, MUFA and PUFA.

Studies using gas chromatography to analyse individual fatty acids in subcutaneous and visceral adipose tissue have documented that PUFA are fairly homogeneously distributed in different adipose tissue depots (subcutaneous abdominal, subcutaneous femoral and visceral) (Seidelin 1995). In contrast, small but statistically significant differences are observed in MUFA and SAFA content of different fat depots, with visceral adipose tissue containing more SAFA than subcutaneous adipose tissue (Seidelin 1995). According to these previous studies, the SAFA-to-MUFA ratio largely explains differences in unsaturation of different adipose tissue depots. In face of this, a probable explanation of the close correlation between adipose and liver fat is that the PUFA profiles are similar in these compartments. Thus differences in the saturation between the compartments would be due to differences in the SAFA-to-MUFA ratio.

Similarities in the fatty acid profile of liver and adipose tissue TG are expected, as these two compartments are linked by trafficking of circulating FAs. Donnelly *et al*. determined using stable isotope labelling that fatty acids for liver TGs are mainly derived from the plasma NEFA pool (Donnelly *et al*. 2005). Other FA sources for liver TG are dietary fat from chylomicrons, de-novo-lipogenesis and recycled circulating triglyceride rich lipoproteins (Postic *et al*. 2008). Liver TG are exported in VLDL particles, which are hydrolyzed by lipoprotein lipase with FA taken up by adipose tissue, thereby forming a continuous loop of FA in liver and adipose tissue (Postic *et al*. 2008).

The significantly higher saturation observed for liver fat compared to adipose tissue fat can be attributed to differences in FA handling in this loop, or to tissue specific handling of FA. Plasma NEFA are mainly derived from adipose tissue by lipolysis (Lewis *et al*. 2002). Hormone sensitive lipase is known to preferentially release long-chain PUFA with little to no differences in preference for MUFA and SAFA release (Donnelly *et al*. 2005, Halliwell *et al*. 1996, Raclot *et al*. 1997), indicating that lipolysis is not a probable explanation for the observed differences in saturation. Spill over from TG hydrolyzed by lipoprotein lipase from triglyceride rich lipoproteins not taken up by adipose tissue can also contribute to plasma NEFA (Binnert *et al*. 1996, Miles *et al*. 2004). In the fasting state the composition of plasma NEFA is more saturated than adipose tissue FA (Jacobsen *et al*. 1983), probably reflecting decreased uptake of saturated fat in adipose tissue and skeletal muscle (Halliwell *et al*. 1996). Whether differences in FA uptake can impact the relative saturation of liver and adipose tissue TG is unclear.

Studies have indicated that adipose tissue and liver may exhibit differences in de-novo-lipogenesis (DNL) (Aarsland *et al*. 1997, Diraison *et al*. 2002), a potential modulator of fat saturation. Recent studies comparing NAFLD patients and healthy controls have shown fasting state DNL is increased in NAFLD by contributing up to 25% of both liver

and VLDL TG as compared to 5 % in VLDL of healthy controls (Hudgins *et al*. 2000, Parks *et al*. 1999). Also adipose tissue has significant capacity for DNL, with deuterium labelling suggesting a 20 % contribution of DNL to adipose tissue TG in healthy subjects, presumably exceeding liver DNL (Strawford *et al*. 2004). Adipose tissue and liver may also be uncoupled in their response to DNL induced by a high-carbohydrate diet (Diraison *et al*. 2003). Recently, adipocyte studies indicated that a high saturated fat content, especially stearic acid 18:0, correlated positively with adipocyte insulin sensitivity (Sjögren *et al*. 2008, Roberts *et al*. 2009) and was attributed to increased DNL (Roberts *et al*. 2009).

Our results on liver fat unsaturation could thus be interpreted as a shift in DNL from adipose tissue to the liver in NAFLD.

6.4 Future aspects

Over the years the composition of tissue triglycerides have been linked with many disorders (Seidelin 1995). However, the observed changes are likely non-specific and difficult to distinguish from normal biological variation. Spectroscopic methods for determining triglyceride composition will accordingly have applications mainly as research tools. Interest in adipose tissue triglyceride composition has recently been reinvigorated, when high saturated fat content was reported to indicate good insulin sensitivity in adipocytes (Roberts *et al*. 2009). With growing evidence linking insulin resistance with T2D and CVD, the methods introduced here can provide new insights into their pathogenesis. The mechanisms behind the increase in adipose tissue ω-3 PUFA content with age are unknown (Bolton-Smith *et al*. 1997). The non-invasive quantitation of adipose tissue ω-3 PUFA content provides new possibilities for conducting research and may shed some light on this issue. Long TE ^{1}H-MRS may also prove useful in determining the link between breast adipose tissue triglyceride composition and breast cancer (He *et al*. 2007). The field of non-invasive spectroscopy is rapidly expanding, with ^{13}C-NMR spectroscopy (Hwang *et al*. 2003) and ultra high field strengths (Ren *et al*. 2008) the next logical steps for improving the *in vivo* analysis of fat composition.

References

AARSLAND, A., CHINKES, D. and WOLFE, R.R., 1997. Hepatic and whole-body fat synthesis in humans during carbohydrate overfeeding. *The American Journal of Clinical Nutrition,* **65**(6), 1774-1782.

ADAM, M., MOSSOBA, M., DAWSON, T., CHEW, M. and WASSERMAN, S., 1999. Comparison of attenuated total reflection infrared spectroscopy to capillary gas chromatography for *trans* fatty acid determination. *Journal of the American Oil Chemists' Society,* **76**(3), 375-378.

ADIELS, M., WESTERBACKA, J., SORO-PAAVONEN, A., HÄKKINEN, A., VEHKAVAARA, S., CASLAKE, M., PACKARD, C., OLOFSSON, S., YKI-JÃRVINEN, H., TASKINEN, M. and BORÉN, J., 2007. Acute suppression of VLDL1 secretion rate by insulin is associated with hepatic fat content and insulin resistance. *Diabetologia,* **50**(11), 2356-2365.

AILHAUD, G., MASSIERA, F., WEILL, P., LEGRAND, P., ALESSANDRI, J. and GUESNET, P., 2006. Temporal changes in dietary fats: Role of n−6 polyunsaturated fatty acids in excessive adipose tissue development and relationship to obesity. *Progress in lipid research,* **45**(3), 203-236.

ALBERTI, K.G.M.M., ZIMMET, P., SHAW, J. and IDF EPIDEMIOLOGY TASK FORCE CONSENSUS GROUP, 2005. The metabolic syndrome--a new worldwide definition. *Lancet,* **366**(9491), 1059-1062.

ANGULO, P., 2002. Nonalcoholic fatty liver disease. *The New England journal of medicine,* **346**(16), 1221-1231.

ARAB, L., 2003. Biomarkers of fat and fatty acid intake. *The Journal of nutrition,* **133 Suppl 3**, 925S-932S.

ARAYA, J., RODRIGO, R., VIDELA, L.A., THIELEMANN, L., ORELLANA, M., PETTINELLI, P. and PONIACHIK, J., 2004. Increase in long-chain polyunsaturated fatty acid n - 6/n - 3 ratio in relation to hepatic steatosis in patients with non-alcoholic fatty liver disease. *Clinical science (London, England : 1979),* **106**(6), 635-643.

BAETEN, V., HOURANT, P., MORALES, M.T. and APARICIO, R., 1998. Oil and Fat Classification by FT-Raman Spectroscopy. *Journal of Agricultural and Food Chemistry,* **46**(7), 2638-2646.

BERRY, E., HIRSCH, J., MOST, J., MCNAMARA, D. and THORNTON, J., 1986. The relationship of dietary fat to plasma lipid levels as studied by factor analysis of adipose tissue fatty acid composition in a free- living population of middle-aged American men. *The American Journal of Clinical Nutrition,* **44**(2), 220-231.

BINNERT, C., PACHIAUDI, C., BEYLOT, M., CROSET, M., COHEN, R., RIOU, J.P. and LAVILLE, M., 1996. Metabolic fate of an oral long-chain triglyceride load in humans. *The American Journal of Physiology*, **270**(3 Pt 1), E445-50.

BLOCH, F., 1946. Nuclear Induction. *Physical Review*, **70**(7-8), 460.

BLOEMBERGEN, N., PURCELL, E.M. and POUND, R.V., 1948. Relaxation Effects in Nuclear Magnetic Resonance Absorption. *Physical Review*, **73**(7), 679.

BOESCH, C., SLOTBOOM, J., HOPPELER, H. and KREIS, R., 1997. In vivo determination of intra-myocellular lipids in human muscle by means of localized ^{1}H-MR-spectroscopy. *Magnetic resonance in medicine*, **37**(4), 484-493.

BOESCH, C., MACHANN, J., VERMATHEN, P. and SCHICK, F., 2006. Role of proton MR for the study of muscle lipid metabolism. *NMR in biomedicine*, **19**(7), 968-988.

BOLTON-SMITH, C., WOODWARD, M. and TAVENDALE, R., 1997. Evidence for age-related differences in the fatty acid composition of human adipose tissue, independent of diet. *European journal of clinical nutrition*, **51**(9), 619-624.

BOTTOMLEY P.A., 1984. Selective volume method for performing localized NMR spectroscopy. *United States Patent* nr. 4480228.

CEN, H. and HE, Y., 2007. Theory and application of near infrared reflectance spectroscopy in determination of food quality. *Trends in Food Science & Technology*, **18**(2), 72-83.

CHRISTIE, W.W., 1989. *Gas Chromatography and Lipids: a Practical Guide.* Ayr Scotland: The Oily Press.

CHRISTY, A.A., EGEBERG, P.K. and ØSTENSEN, E.T., 2003. Simultaneous quantitative determination of isolated *trans* fatty acids and conjugated linoleic acids in oils and fats by chemometric analysis of the infrared profiles. *Vibrational Spectroscopy*, **33**(1-2), 37-48.

COBBOLD, J.F., TAYLOR-ROBINSON, S.D. and COX, I.J., 2008. In vitro proton magnetic resonance spectroscopy of liver tissue informs in vivo hepatic proton magnetic resonance spectroscopy studies. *Hepatology (Baltimore, Md.)*, **48**(3), 1016; author reply 1016-7.

CONSIDINE, R.V., SINHA, M.K., HEIMAN, M.L., KRIAUCIUNAS, A., STEPHENS, T.W., NYCE, M.R., OHANNESIAN, J.P., MARCO, C.C., MCKEE, L.J., BAUER, T.L. and CARO, J.F., 1996. Serum Immunoreactive-Leptin Concentrations in Normal-Weight and Obese Humans. *New England Journal of Medicine*, **334**(5), 292-295.

DE GRAAF, R.A., 1998. *In vivo NMR spectroscopy: Principles and Techniques.* West Sussex, England: John Wiley & Sons, Ltd.

DE JUAN, A., VANDER HEYDEN, Y., TAULER, R. and MASSART, D.L., 1997. Assessment of new constraints applied to the alternating least squares method. *Analytica Chimica Acta*, **346**(3), 307-318.

DIRAISON, F., DUSSERRE, E., VIDAL, H., SOTHIER, M. and BEYLOT, M., 2002. Increased hepatic lipogenesis but decreased expression of lipogenic gene in adipose tissue in human obesity. *American journal of physiology.Endocrinology and metabolism*, **282**(1), E46-51.

DIRAISON, F., YANKAH, V., LETEXIER, D., DUSSERRE, E., JONES, P. and BEYLOT, M., 2003. Differences in the regulation of adipose tissue and liver lipogenesis by carbohydrates in humans. *Journal of lipid research*, **44**(4), 846-853.

DONNELLY, K.L., SMITH, C.I., SCHWARZENBERG, S.J., JESSURUN, J., BOLDT, M.D. and PARKS, E.J., 2005. Sources of fatty acids stored in liver and secreted via lipoproteins in patients with nonalcoholic fatty liver disease. *The Journal of clinical investigation*, **115**(5), 1343-1351.

DREWNOWSKI, A., 2007. The Real Contribution of Added Sugars and Fats to Obesity. *Epidemiologic Reviews*, **29**(1), 160-171.

EVANS, K., BURDGE, G.C., WOOTTON, S.A., CLARK, M.L. and FRAYN, K.N., 2002. Regulation of Dietary Fatty Acid Entrapment in Subcutaneous Adipose Tissue and Skeletal Muscle. *Diabetes*, **51**(9), 2684-2690.

FABIAN, H., LASCH, P., BOESE, M. and HAENSCH, W., 2002. Mid-IR microspectroscopic imaging of breast tumor tissue sections. *Biopolymers*, **67**(4-5), 354-357.

FANG, X. and SWEENEY, G., 2006. Mechanisms regulating energy metabolism by adiponectin in obesity and diabetes. *Biochemical Society Transactions.*, **34**(Pt 5), 798-801.

FIELD, A.E., WILLETT, W.C., LISSNER, L. and COLDITZ, G.A., 2007. Dietary Fat and Weight Gain Among Women in the Nurses' Health Study. *Obesity*, **15**(4), 967-976.

FRAHM, J., MERBOLDT, K. and HÄNICKE, W., 1987.. Localized proton spectroscopy using stimulated echoes. *Journal of Magnetic Resonance (1969)*, **72**(3), 502-508.

FRITSCHE, J., STEINHART, H., MOSSOBA, M.M., YURAWECZ, M.P., SEHAT, N. and KU, Y., 1998. Rapid determination of *trans*-fatty acids in human adipose tissue. Comparison of attenuated total reflection infrared spectroscopy and gas chromatography. *Journal of chromatography.B, Biomedical sciences and applications*, **705**(2), 177-182.

GEMPERLINE, P., ed, 2006. *Practical Guide to Chemometrics*, 2nd edn. Boka Raton FL: CRC Press.

GOORMAGHTIGH, E., RAUSSENS, V. and RUYSSCHAERT, J., 1999. Attenuated total reflection infrared spectroscopy of proteins and lipids in biological membranes. *Biochimica et Biophysica Acta (BBA) - Reviews on Biomembranes,* **1422**(2), 105-185.

GOUDAPPEL, G.J.W., VAN DUYNHOVEN, J.P.M. and MOOREN, M.M.W., 2001. Measurement of Oil Droplet Size Distributions in Food Oil/Water Emulsions by Time Domain Pulsed Field Gradient NMR. *Journal of colloid and interface science,* **239**(2), 535-542.

GRIFFITHS, P. and DE HASETH, J.A., 1986. *Fourier Transform Infrared Spectrometry.* Hoboken, New Jersey: John Wiley & Sons, Inc.

GUILLÉN, M.D. and CABO, N., 1997. Infrared spectroscopy in the study of edible oils and fats. *Journal of the science of food and agriculture,* **75**(1), 1-11.

GUILLÉN, M.D. and CABO, N., 1999. Usefulness of the Frequency Data of the Fourier Transform Infrared Spectra To Evaluate the Degree of Oxidation of Edible Oils. *Journal of Agricultural and Food Chemistry,* **47**(2), 709-719.

GUILLÉN, M.D. and CABO, N., 1998. Relationships between the Composition of Edible Oils and Lard and the Ratio of the Absorbance of Specific Bands of Their Fourier Transform Infrared Spectra. Role of Some Bands of the Fingerprint Region. *Journal of Agricultural and Food Chemistry,* **46**(5), 1788-1793.

GUILLÉN, M.D. and RUIZ, A., 2003. Edible oils: discrimination by ^{1}H nuclear magnetic resonance. *Journal of the science of food and agriculture,* **83**(4), 338-346.

HAHN, E.L., 1950. Spin Echoes. *Physical Review,* **80**(4), 580.

HAKUMAKI, J.M., POPTANI, H., SANDMAIR, A., YLÄ-HERTTUALA, S. and KAUPPINEN, R.A., 1999. ^{1}H MRS detects polyunsaturated fatty acid accumulation during gene therapy of glioma: Implications for the in vivo detection of apoptosis. *Nature medicine,* **5**(11), 1323-1327.

HALLIWELL, K.J., FIELDING, B.A., SAMRA, J.S., HUMPHREYS, S.M. and FRAYN, K.N., 1996. Release of individual fatty acids from human adipose tissue in vivo after an overnight fast. *Journal of lipid research,* **37**(9), 1842-1848.

HE, Q., SHKARIN, P., HOOLEY, R.J., LANNIN, D.R., WEINREB, J.C. and BOSSUYT, V.I.J., 2007. In vivo MR spectroscopic imaging of polyunsaturated fatty acids (PUFA) in healthy and cancerous breast tissues by selective multiple-quantum coherence transfer (Sel-MQC): A preliminary study. *Magnetic Resonance in Medicine,* **58**(6), 1079-1085.

HUDGINS, L.C., HELLERSTEIN, M.K., SEIDMAN, C.E., NEESE, R.A., TREMAROLI, J.D. and HIRSCH, J., 2000. Relationship between carbohydrate-induced hypertriglyceridemia and fatty acid synthesis in lean and obese subjects. *Journal of lipid research,* **41**(4), 595-604.

HUDGINS, L.C., HIRSCH, J. and EMKEN, E.A., 1991. Correlation of isomeric fatty acids in human adipose tissue with clinical risk factors for cardiovascular disease. *The American Journal of Clinical Nutrition,* **53**(2), 474-482.

HWANG, J., BLUML, S., LEAF, A. and ROSS, B.D., 2003. *In vivo* characterization of fatty acids in human adipose tissue using natural abundance ^{1}H decoupled ^{13}C MRS at 1.5 T: clinical applications to dietary therapy. *NMR in biomedicine,* **16**(3), 160-167.

ISMAIL, A., VAN, D.V., EMO, G. and SEDMAN, J., 1993. Rapid quantitative determination of free fatty acids in fats and oils by fourier transform infrared spectroscopy. *Journal of the American Oil Chemists' Society,* **70**(4), 335-341.

JACOBSEN, B.K., TRYGG, K., HJERMANN, I., THOMASSEN, M.S., REAL, C. and NORUM, K.R., 1983. Acyl pattern of adipose tissue triglycerides, plasma free fatty acids, and diet of a group of men participating in a primary coronary prevention program (the Oslo Study). *The American Journal of Clinical Nutrition,* **38**(6), 906-913.

JOHNSON, N.A., WALTON, D.W., SACHINWALLA, T., THOMPSON, C.H., SMITH, K., RUELL, P.A., STANNARD, S.R. and GEORGE, J., 2008. Noninvasive assessment of hepatic lipid composition: Advancing understanding and management of fatty liver disorders. *Hepatology (Baltimore, Md.),* **47**(5), 1513-1523.

KNOTHE, G. and KENAR, J.A., 2004. Determination of the fatty acid profile by ^{1}H-NMR spectroscopy. *European Journal of Lipid Science and Technology,* **106**(2), 88-96.

KOH-BANERJEE, P., CHU, N., SPIEGELMAN, D., ROSNER, B., COLDITZ, G., WILLETT, W. and RIMM, E., 2003. Prospective study of the association of changes in dietary intake, physical activity, alcohol consumption, and smoking with 9-y gain in waist circumference among 16 587 US men. *The American Journal of Clinical Nutrition,* **78**(4), 719-727.

KOPELMAN, P.G., 2000. Obesity as a medical problem. *Nature,* **404**(6778), 635-643.

LAATIKAINEN, R., NIEMITZ, M., MALAISSE, W.J., BIESEMANS, M. and WILLEM, R., 1996. A computational strategy for the deconvolution of NMR spectra with multiplet structures and constraints: analysis of overlapping 13C-2H multiplets of 13C enriched metabolites from cell suspensions incubated in deuterated media. *Magnetic resonance in medicine,* **36**(3), 359-365.

LAHRECH, H., ZOULA, S., FARION, R., RÉMY, C. and DÉCORPS, M., 2001. In vivo measurement of the size of lipid droplets in an intracerebral glioma in the rat. *Magnetic Resonance in Medicine,* **45**(3), 409-414.

LAI, Y.W., KEMSLEY, E.K. and WILSON, R.H., 1994. Potential of Fourier Transform Infrared Spectroscopy for the Authentication of Vegetable Oils. *Journal of Agricultural and Food Chemistry,* **42**(5), 1154-1159.

LE, K., ITH, M., KREIS, R., FAEH, D., BORTOLOTTI, M., TRAN, C., BOESCH, C. and TAPPY, L., 2009. Fructose overconsumption causes dyslipidemia and ectopic lipid deposition in healthy subjects with and without a family history of type 2 diabetes. *The American Journal of Clinical Nutrition,* **89**(6), 1760-1765.

LEWIS, G.F., CARPENTIER, A., ADELI, K. and GIACCA, A., 2002. Disordered fat storage and mobilization in the pathogenesis of insulin resistance and type 2 diabetes. *Endocrine reviews,* **23**(2), 201-229.

LI, H., VAN, D.V., ISMAIL, A., SEDMAN, J., COX, R., SIMARD, C. and BUIJS, H., 2000. Discrimination of edible oil products and quantitative determination of their iodine value by Fourier transform near-infrared spectroscopy. *Journal of the American Oil Chemists' Society,* **77**(1), 29-36.

LICHTMAN, S., PISARSKA, K., BERMAN, E., PESTONE, M., DOWLING, H., OFFENBACHER, E., WEISEL, H., HESHKA, S., MATTHEWS, D. and HEYMSFIELD, S., 1992. Discrepancy between self-reported and actual caloric intake and exercise in obese subjects. *New England Journal of Medicine,* **327**(27), 1893-1898.

LIE KEN JIE, M.S.F. and LAM, C.C., 1995. ^{1}H-Nuclear magnetic resonance spectroscopic studies of saturated, acetylenic and ethylenic triacylglycerols. *Chemistry and physics of lipids,* **77**(2), 155-171.

LUNATI, E., FARACE, P., NICOLATO, E., RIGHETTI, C., MARZOLA, P., SBARBATI, A. and OSCULATI, F., 2001. Polyunsaturated fatty acids mapping by ^{1}H MR-chemical shift imaging. *Magnetic Resonance in Medicine,* **46**(5), 879-883.

MANSON, J.E., COLDITZ, G.A., STAMPFER, M.J., WILLETT, W.C., ROSNER, B., MONSON, R.R., SPEIZER, F.E. and HENNEKENS, C.H., 1990. A Prospective Study of Obesity and Risk of Coronary Heart Disease in Women. *New England Journal of Medicine,* **322**(13), 882-889.

MIERISOVÁ, S., BOOGAART, A.V.D., TKÁC, I., HECKE, P.V., VANHAMME, L. and LIPTAJ, T., 1998. New approach for quantitation of short echo time *in vivo* ^{1}H MR spectra of brain using AMARES. *NMR in biomedicine,* **11**(1), 32-39.

MILES, J.M., PARK, Y.S., WALEWICZ, D., RUSSELL-LOPEZ, C., WINDSOR, S., ISLEY, W.L., COPPACK, S.W. and HARRIS, W.S., 2004. Systemic and forearm triglyceride metabolism: fate of lipoprotein lipase-generated glycerol and free fatty acids. *Diabetes,* **53**(3), 521-527.

MOSSOBA, M., KRAMER, J., MILOSEVIC, V., MILOSEVIC, M. and AZIZIAN, H., 2007. Interference of Saturated Fats in the Determination of Low Levels of *trans* Fats (below 0.5%) by Infrared Spectroscopy. *Journal of the American Oil Chemists' Society,* **84**(4), 339-342.

MOZAFFARIAN, D., KATAN, M.B., ASCHERIO, A., STAMPFER, M.J. and WILLETT, W.C., 2006. *Trans* Fatty Acids and Cardiovascular Disease. *New England Journal of Medicine,* **354**(15), 1601-1613.

NAUMANN, D., HELM, D. and LABISCHINSKI, H., 1991. Microbiological characterizations by FT-IR spectroscopy. *Nature,* **351**(6321), 81-82.

OOSTENDORP, M., ENGELKE, U.F., WILLEMSEN, M.A. and WEVERS, R.A., 2006. Diagnosing Inborn Errors of Lipid Metabolism with Proton Nuclear Magnetic Resonance Spectroscopy. *Clinical chemistry,* **52**(7), 1395-1405.

OZEN, B.F. and MAUER, L.J., 2002. Detection of Hazelnut Oil Adulteration Using FT-IR Spectroscopy. *Journal of Agricultural and Food Chemistry,* **50**(14), 3898-3901.

PARKS, E.J., KRAUSS, R.M., CHRISTIANSEN, M.P., NEESE, R.A. and HELLERSTEIN, M.K., 1999. Effects of a low-fat, high-carbohydrate diet on VLDL-triglyceride assembly, production, and clearance. *The Journal of clinical investigation,* **104**(8), 1087-1096.

PIJNAPPEL, W.W.F., VAN DEN BOOGAART, A., DE BEER, R. and VAN ORMONDT, D., 1992. SVD-based quantification of magnetic resonance signals. *Journal of Magnetic Resonance (1969),* **97**(1), 122-134.

POSTIC, C. and GIRARD, J., 2008. Contribution of de novo fatty acid synthesis to hepatic steatosis and insulin resistance: lessons from genetically engineered mice. *The Journal of clinical investigation,* **118**(3), 829-838.

PROVENCHER, S., 2008. *LCmodel & LCMgui User's Manual, Version 6.2-1*. http://s-provencher.com/pages/lcmodel.shtml, downloaded January 15th 2009.

PURI, P., BAILLIE, R.A., WIEST, M.M., MIRSHAHI, F., CHOUDHURY, J., CHEUNG, O., SARGEANT, C., CONTOS, M.J. and SANYAL, A.J., 2007. A lipidomic analysis of nonalcoholic fatty liver disease. *Hepatology (Baltimore, Md.),* **46**(4), 1081-1090.

QUERLEUX, B., CORNILLON, C., JOLIVET, O. and BITTOUN, J., 2002. Anatomy and physiology of subcutaneous adipose tissue by in vivo magnetic resonance imaging and spectroscopy: relationships with sex and presence of cellulite. *Skin research and technology,* **8**(2), 118-124.

RACLOT, T., LANGIN, D., LAFONTAN, M. and GROSCOLAS, R., 1997. Selective release of human adipocyte fatty acids according to molecular structure. *The Biochemical journal,* **324** (Pt 3), 911-915.

RAMSEY, N.F. and PURCELL, E.M., 1952. Interactions between Nuclear Spins in Molecules. *Physical Review,* **85**(1), 143.

RATINEY, H., SDIKA, M., COENRADIE, Y., CAVASSILA, S., ORMONDT, D.V. and GRAVERON-DEMILLY, D., 2005. Time-domain semi-parametric estimation based on a metabolite basis set. *NMR in biomedicine,* **18**(1), 1-13.

REAVEN, G.M., 1988. Banting lecture 1988. Role of insulin resistance in human disease. *Diabetes,* **37**(12), 1595-1607.

REN, J., DIMITROV, I., SHERRY, A.D. and MALLOY, C.R., 2008. Composition of adipose tissue and marrow fat in humans by ^{1}H NMR at 7 Tesla. *Journal of lipid research,* **49**(9), 2055-2062.

ROBERTS, R., HODSON, L., DENNIS, A., NEVILLE, M., HUMPHREYS, S., HARNDEN, K., MICKLEM, K. and FRAYN, K., 2009. Markers of de novo lipogenesis in adipose tissue: associations with small adipocytes and insulin sensitivity in humans. *Diabetologia,* **52**(5), 882-890.

SACCHI, R., ADDEO, F. and PAOLILLO, L., 1997. ^{1}H and ^{13}C NMR of virgin olive oil. An overview. *Magnetic Resonance in Chemistry,* **35**(13), S133-S145.

SCHICK, F., EISMANN, B., JUNG, W.I., BONGERS, H., BUNSE, M. and LUTZ, O., 1993. Comparison of localized proton NMR signals of skeletal muscle and fat tissue in vivo: two lipid compartments in muscle tissue. *Magnetic resonance in medicine,* **29**(2), 158-167.

SCHICK, F., 1996. Bone marrow NMR in vivo. *Progress in Nuclear Magnetic Resonance Spectroscopy,* **29**(3-4), 169-227.

SCHOONOVER, J.R., MARX, R. and ZHANG, S.L., 2003. Multivariate curve resolution in the analysis of vibrational spectroscopy data files. *Applied Spectroscopy,* **57**(5), 154A-170A.

SEIDELIN, K.N., 1995. Fatty acid composition of adipose tissue in humans. Implications for the dietary fat-serum cholesterol-CHD issue. *Progress in lipid research,* **34**(3), 199-217.

SEPPÄLÄ-LINDROOS, A., VEHKAVAARA, S., HÄKKINEN, A., GOTO, T., WESTERBACKA, J., SOVIJÄRVI, A., HALAVAARA, J. and YKI-JÄRVINEN, H., 2002. Fat Accumulation in the Liver Is Associated with Defects in Insulin Suppression of Glucose Production and Serum Free Fatty Acids Independent of Obesity in Normal Men. *Journal of Clinical Endocrinology & Metabolism,* **87**(7), 3023-3028.

SJÖGREN, P., SIERRA-JOHNSON, J., GERTOW, K., ROSELL, M., VESSBY, B., DE FAIRE, U., HAMSTEN, A., HELLENIUS, M.-. and FISHER, R.M., 2008. Fatty acid desaturases in human adipose tissue: relationships between gene expression, desaturation indexes and insulin resistance. *Diabetologia,* **51**(2), 328-335.

SKOCH, A., JÍRU, F., DEZORTOVÁ, M., KRUSINOVÁ, E., KRATOCHVÍLOVÁ, S., PELIKÁNOVÁ, T., GRODD, W. and HÁJEK, M., 2006. Intramyocellular lipid quantification from ^{1}H long echo time spectra at 1.5 and 3 T by means of the LCModel technique. *Journal of magnetic resonance imaging*, **23**(5), 728-735.

SPADARO, L., MAGLIOCCO, O., SPAMPINATO, D., PIRO, S., OLIVERI, C., ALAGONA, C., PAPA, G., RABUAZZO, A.M. and PURRELLO, F., 2008. Effects of n-3 polyunsaturated fatty acids in subjects with nonalcoholic fatty liver disease. *Digestive and Liver Disease*, **40**(3), 194-199.

STANHOPE, K.L., SCHWARZ, J.M., KEIM, N.L., GRIFFEN, S.C., BREMER, A.A., GRAHAM, J.L., HATCHER, B., COX, C.L., DYACHENKO, A., ZHANG, W., MCGAHAN, J.P., SEIBERT, A., KRAUSS, R.M., CHIU, S., SCHAEFER, E.J., AI, M., OTOKOZAWA, S., NAKAJIMA, K., NAKANO, T., BEYSEN, C., HELLERSTEIN, M.K., BERGLUND, L. and HAVEL, P.J., 2009. Consuming fructose-sweetened, not glucose-sweetened, beverages increases visceral adiposity and lipids and decreases insulin sensitivity in overweight/obese humans. *The Journal of clinical investigation*, **119**(5), 1322-1334.

STRAWFORD, A., ANTELO, F., CHRISTIANSEN, M. and HELLERSTEIN, M.K., 2004. Adipose tissue triglyceride turnover, de novo lipogenesis, and cell proliferation in humans measured with 2H2O. *American journal of physiology.Endocrinology and metabolism*, **286**(4), E577-88.

STROBEL, K., VAN DEN HOFF, J. and PIETZSCH, J., 2008. Localized proton magnetic resonance spectroscopy of lipids in adipose tissue at high spatial resolution in mice in vivo. *Journal of lipid research*, **49**(2), 473-480.

SULLIVAN, S., 2010. Implications of diet on nonalcoholic fatty liver disease. *Current opinion in gastroenterology*, **26**(2), 160-164.

SZCZEPANIAK, L.S., BABCOCK, E.E., SCHICK, F., DOBBINS, R.L., GARG, A., BURNS, D.K., MCGARRY, J.D. and STEIN, D.T., 1999. Measurement of intracellular triglyceride stores by H spectroscopy: validation in vivo. *The American Journal of Physiology*, **276**(5 Pt 1), E977-89.

SZCZEPANIAK, L.S., NURENBERG, P., LEONARD, D., BROWNING, J.D., REINGOLD, J.S., GRUNDY, S., HOBBS, H.H. and DOBBINS, R.L., 2005. Magnetic resonance spectroscopy to measure hepatic triglyceride content: prevalence of hepatic steatosis in the general population. *American journal of physiology.Endocrinology and metabolism*, **288**(2), E462-8.

SZENDROEDI, J. and RODEN, M., 2009. Ectopic lipids and organ function. *Current opinion in.lipidology*, **20**(1), 50-56.

TAULER, R., SMILDE, A. and KOWALSKI, B., 1995. Selectivity, local rank, three-way data analysis and ambiguity in multivariate curve resolution. *Journal of Chemometrics*, **9**(1), 31-58.

VAN DE VOORT, F.R., SEDMAN, J. and RUSSIN, T., 2001. Lipid analysis by vibrational spectroscopy. *European Journal of Lipid Science and Technology*, **103**(12), 815-826.

VANHAMME, L., SUNDIN, T., HECKE, P.V. and HUFFEL, S.V., 2001. MR spectroscopy quantitation: a review of time-domain methods. *NMR in biomedicine*, **14**(4), 233-246.

VANHAMME, L., VAN DEN BOOGAART, A. and VAN HUFFEL, S., 1997. Improved Method for Accurate and Efficient Quantification of MRS Data with Use of Prior Knowledge. *Journal of Magnetic Resonance*, **129**(1), 35-43.

VELAN, S.S., DURST, C., LEMIEUX, S.K., RAYLMAN, R.R., SRIDHAR, R., SPENCER, R.G., HOBBS, G.R. and THOMAS, M.A., 2007. Investigation of muscle lipid metabolism by localized one- and two-dimensional MRS techniques using a clinical 3T MRI/MRS scanner. *Journal of Magnetic Resonance Imaging*, **25**(1), 192-199.

VESSBY, B., UNSITUPA, M., HERMANSEN, K., RICCARDI, G., RIVELLESE, A.A., TAPSELL, L.C., NÄLSÉN, C., BERGLUND, L., LOUHERANTA, A., RASMUSSEN, B.M., CALVERT, G.D., MAFFETONE, A., PEDERSEN, E., GUSTAFSSON, I.B., STORLIEN, L.H. and KANWU STUDY, 2001. Substituting dietary saturated for monounsaturated fat impairs insulin sensitivity in healthy men and women: The KANWU Study. *Diabetologia*, **44**(3), 312-319.

WAJCHENBERG, B.L., 2000. Subcutaneous and visceral adipose tissue: their relation to the metabolic syndrome. *Endocrine reviews*, **21**(6), 697-738.

WESTERBACKA, J., LAMMI, K., HÄKKINEN, A., RISSANEN, A., SALMINEN, I., ARO, A. and YKI-JÄRVINEN, H., 2005. Dietary Fat Content Modifies Liver Fat in Overweight Nondiabetic Subjects. *Journal of Clinical Endocrinology & Metabolism*, **90**(5), 2804-2809.

WILLKER, W. and LEIBFRITZ, D., 1998. Assignment of mono- and polyunsaturated fatty acids in lipids of tissues and body fluids. *Magnetic Resonance in Chemistry*, **36**(S1), S79-S84.

YANG, H., IRUDAYARAJ, J. and PARADKAR, M.M., 2005. Discriminant analysis of edible oils and fats by FTIR, FT-NIR and FT-Raman spectroscopy. *Food Chemistry*, **93**(1), 25-32.

YEUNG, D.K.W., GRIFFITH, J.F., ANTONIO, G.E., LEE, F.K.H., WOO, J. and LEUNG, P.C., 2005. Osteoporosis is associated with increased marrow fat content and decreased marrow fat unsaturation: A proton MR spectroscopy study. *Journal of Magnetic Resonance Imaging*, **22**(2), 279-285.

YOSHIDA, S. and YOSHIDA, H., 2004. Noninvasive analyses of polyunsaturated fatty acids in human oral mucosa in vivo by Fourier-transform infrared spectroscopy. *Biopolymers,* **74**(5), 403-412.

ZIMMERMANN, R., STRAUSS, J.G., HAEMMERLE, G., SCHOISWOHL, G., BIRNER-GRUENBERGER, R., RIEDERER, M., LASS, A., NEUBERGER, G., EISENHABER, F., HERMETTER, A. and ZECHNER, R., 2004. Fat Mobilization in Adipose Tissue Is Promoted by Adipose Triglyceride Lipase. *Science,* **306**(5700), 1383-1386.